

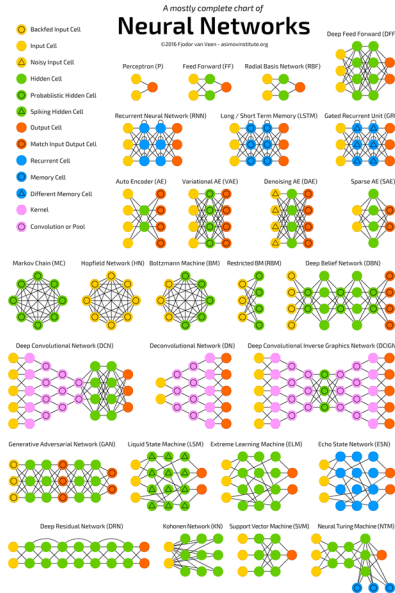
Applying Artificial Intelligence to Accelerators

Alexander Scheinker
(ascheink@lanl.gov)

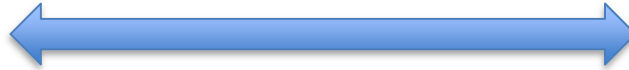
IPAC 2018



Artificial Intelligence: Machines Tuning Themselves

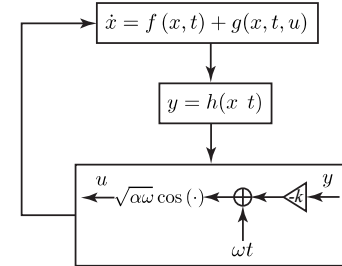
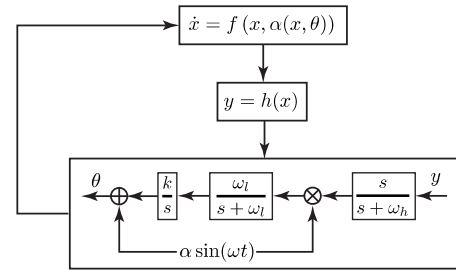


Ocelot optimization and tuning framework (DESY and LCLS)



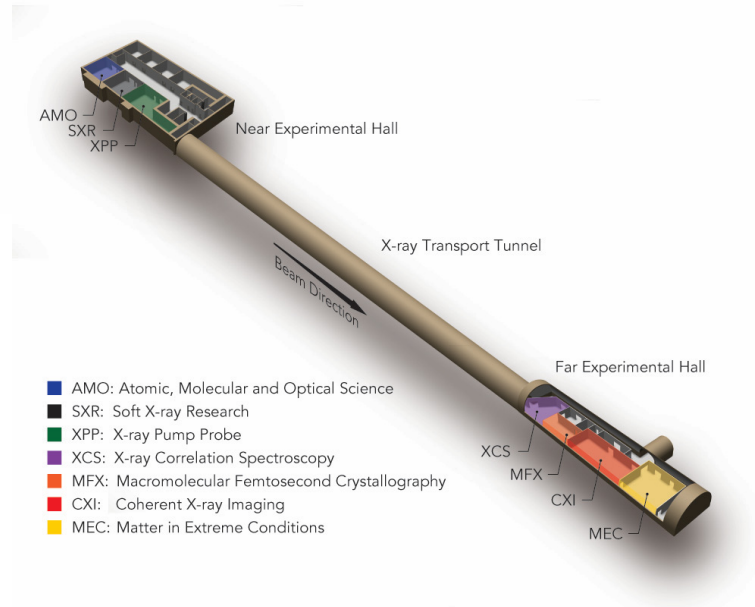
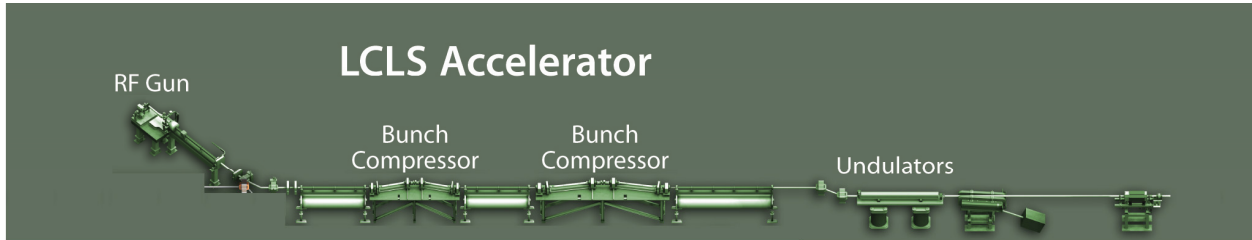
Surrogate models
 Big data
 Global tuning
 Anomaly detection

Adaptive Feedback

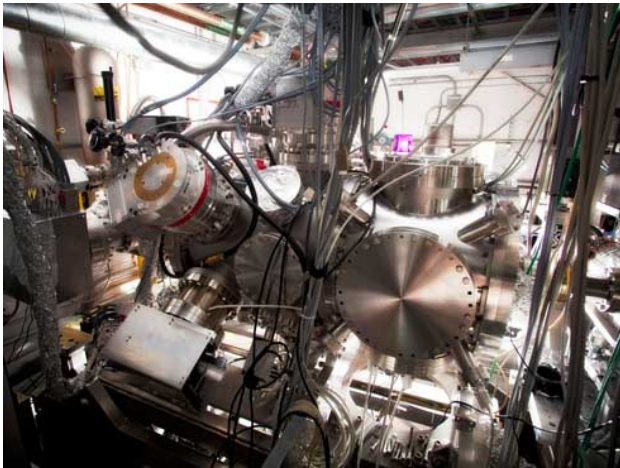


Virtual diagnostics
 Real time feedback
 Optimization
 Phase space tuning

Motivation



AMO



Atomic, Molecular & Optical Science

Soft X-rays for intense ultra short pulses.
Gaseous targets of atoms, molecules, and
nanoscale objects: protein crystals or viruses.

Photon energy: 0.48 – 2 keV

Pulse duration: 35 – 300 fs

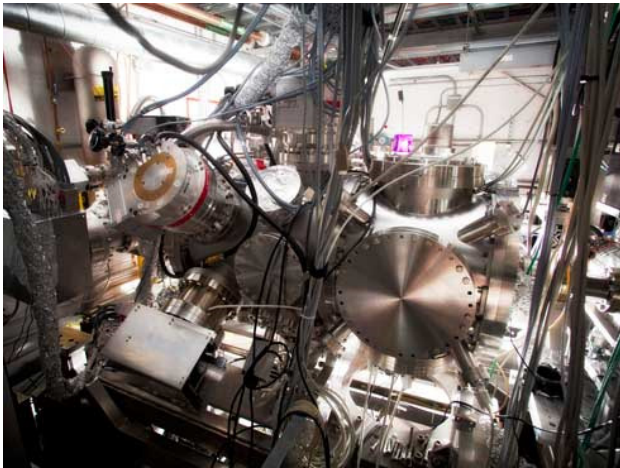
Low charge mode pulse duration: No

Pulse energy: 1 – 20 mJ @ 266 - 800 nm

Max energy adjustment factor: 4.2

Low charge mode: No

AMO



Atomic, Molecular & Optical Science

Soft X-rays for intense ultra short pulses.
Gaseous targets of atoms, molecules, and
nanoscale objects: protein crystals or viruses.

Photon energy: **0.48 – 2 keV**

Pulse duration: **35 – 300 fs**

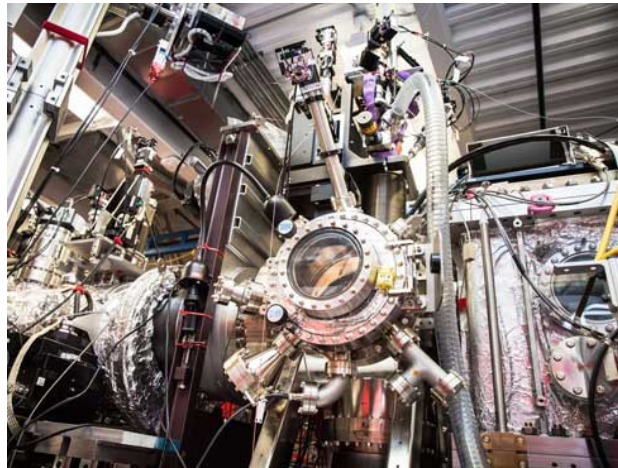
Low charge mode pulse duration: **No**

Pulse energy: **1 – 20 mJ @ 266 - 800 nm**

Max energy adjustment factor: **4.2**

Low charge mode: **No**

CXI



Coherent X-ray imaging

Brilliant hard X-ray pulses for coherent
diffractive imaging (CDI). Ultra short pulses for
“Diffraction-Before-Destruction” experiments.

Photon energy: **5 – 12 keV**

Pulse duration: **40 – 300 fs**

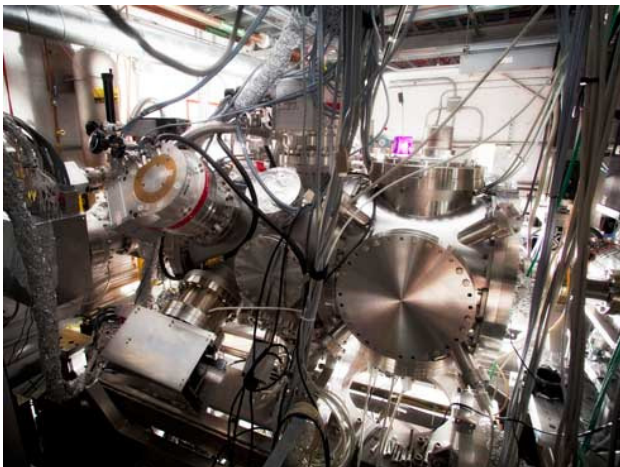
Low charge mode pulse duration: **<10 fs**

Pulse energy: **1 – 3 mJ**

Max energy adjustment factor: **2.4**

Low charge mode: **Yes**

AMO



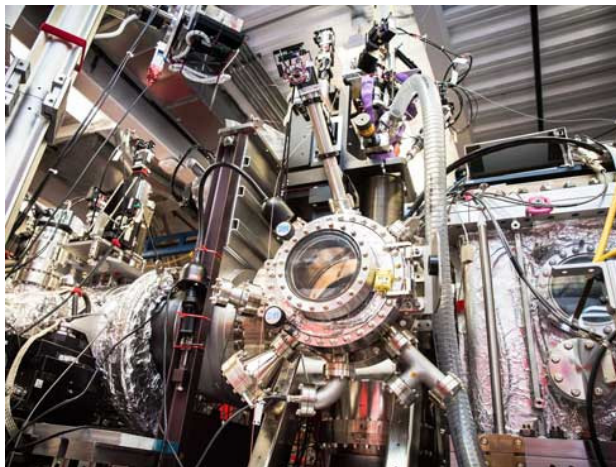
Atomic, Molecular & Optical Science

Soft X-rays for intense ultra short pulses.
Gaseous targets of atoms, molecules, and
nanoscale objects: protein crystals or viruses.

Photon energy: **0.48 – 2 keV**
Pulse duration: **35 – 300 fs**
Low charge mode pulse duration: **No**
Pulse energy: **1 – 20 mJ @ 266 - 800 nm**

Max energy adjustment factor: **4.2**
Low charge mode: **No**

CXI



Coherent X-ray imaging

Brilliant hard X-ray pulses for coherent
diffractive imaging (CDI). Ultra short pulses for
“Diffraction-Before-Destruction” experiments.

Photon energy: **5 – 12 keV**
Pulse duration: **40 – 300 fs**
Low charge mode pulse duration: **<10 fs**
Pulse energy: **1 – 3 mJ**

Max energy adjustment factor: **2.4**
Low charge mode: **Yes**

MEC



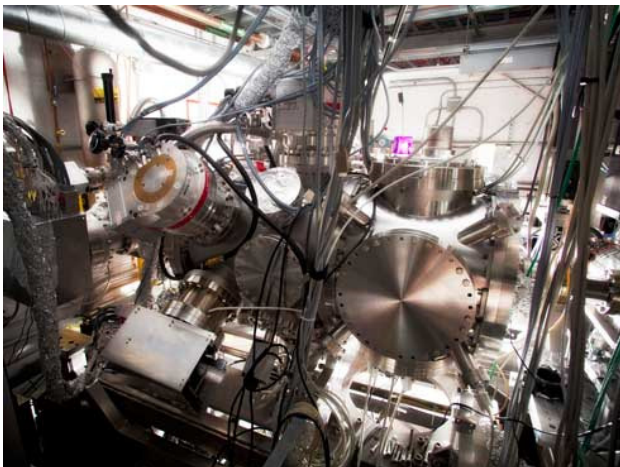
Matter in Extreme Conditions

High peak brightness, ultra short pulses of
tunable energy X-rays for studying the transient
behavior of matter in extreme conditions.

Photon energy: **2.5 – 12 keV**
Pulse duration: **10 – 300 fs**
Low charge mode pulse duration: **<10 fs**
Pulse energy: **1 – 3 mJ**

Max energy adjustment factor: **4.8**
Low charge mode: **Yes**

AMO



Atomic, Molecular & Optical Science

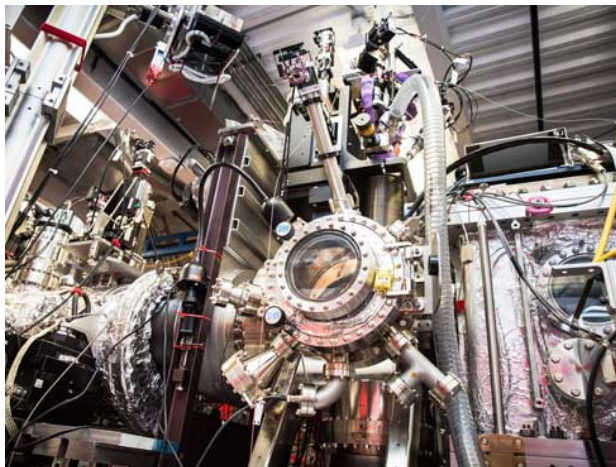
Soft X-rays for intense ultra short pulses.
Gaseous targets of atoms, molecules, and
nanoscale objects: protein crystals or viruses.

Photon energy: **0.48 – 2 keV**
Pulse duration: **35 – 300 fs**
Low charge mode pulse duration: **No**
Pulse energy: **1 – 20 mJ @ 266 - 800 nm**

Max energy adjustment factor: **4.2**
Low charge mode: **No**

Low charge mode: Lower charge per bunch allows for tighter compression without destroying the electron beam's phase space. Originally studying for accelerating 0.02 nC bunches instead of 1 nC.

CXI



Coherent X-ray imaging

Brilliant hard X-ray pulses for coherent
diffractive imaging (CDI). Ultra short pulses for
“Diffraction-Before-Destruction” experiments.

Photon energy: **5 – 12 keV**
Pulse duration: **40 – 300 fs**
Low charge mode pulse duration: **<10 fs**
Pulse energy: **1 – 3 mJ**

Max energy adjustment factor: **2.4**
Low charge mode: **Yes**

MEC



Matter in Extreme Conditions

High peak brightness, ultra short pulses of
tunable energy X-rays for studying the transient
behavior of matter in extreme conditions.

Photon energy: **2.5 – 12 keV**
Pulse duration: **10 – 300 fs**
Low charge mode pulse duration: **<10 fs**
Pulse energy: **1 – 3 mJ**

Max energy adjustment factor: **4.8**
Low charge mode: **Yes**

Need to quickly switch between various beam/light parameters

No such look up table, or button exists

From the FAQ for users on the LCLS website:

1) What is the photon energy range which LCLS can provide and how long does it take to switch?

Answer :

(8/25/16) LCLS Machine Phys.

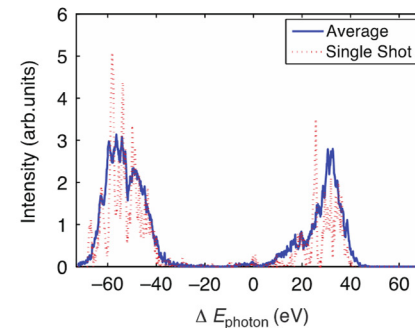
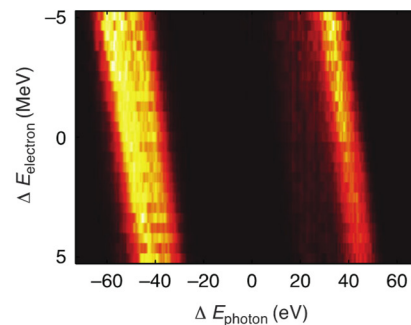
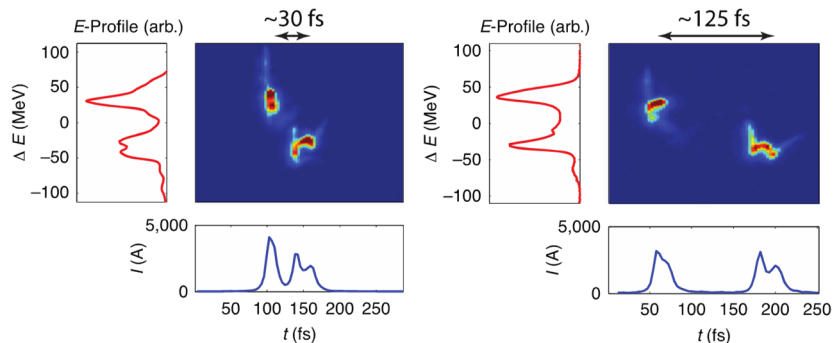
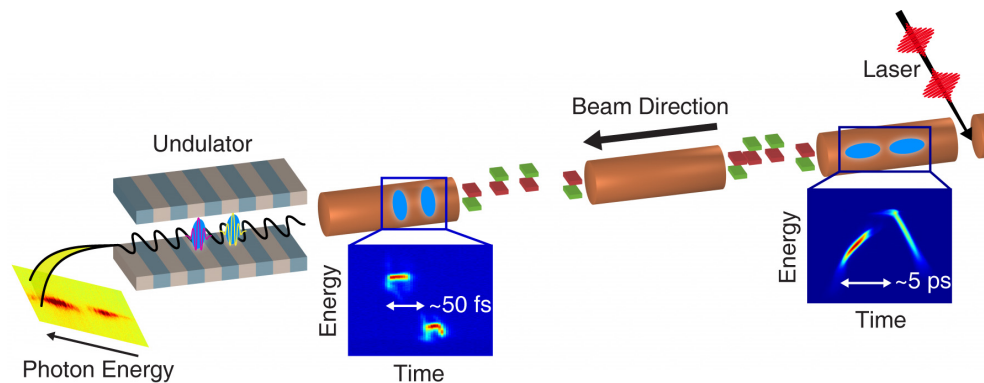
At present, the available photon energy range is 270 eV up to 10 keV. Photon energies as high as 12.8 keV may be reached with advanced notice and reduced reliability.

Factor of > 37

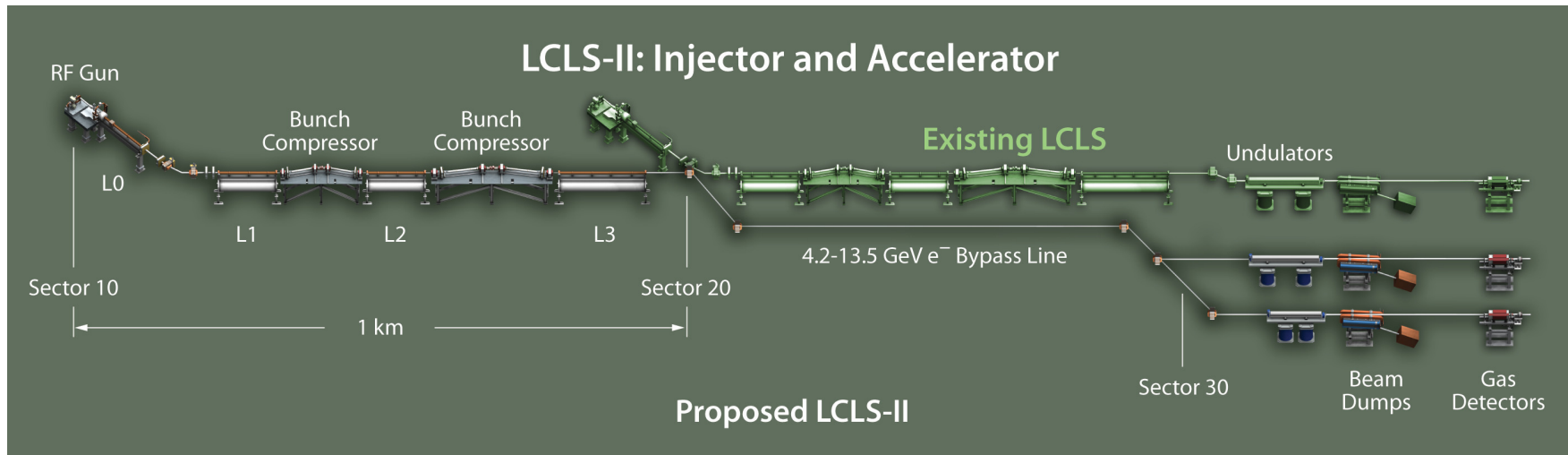


Energy changes can require anywhere from 5 minutes (small energy adjustments of 5-50%) to 45 minutes (energy adjustments of a factor of 2-3). In addition, some accelerator tuning may be required in order to re-establish the full x-ray pulse energy (e.g., to achieve more than 2 mJ may require another hour or more). This retuning is generally faster when the energy is increased rather than decreased. Please ask the operator for a time estimate when requesting photon energy changes.

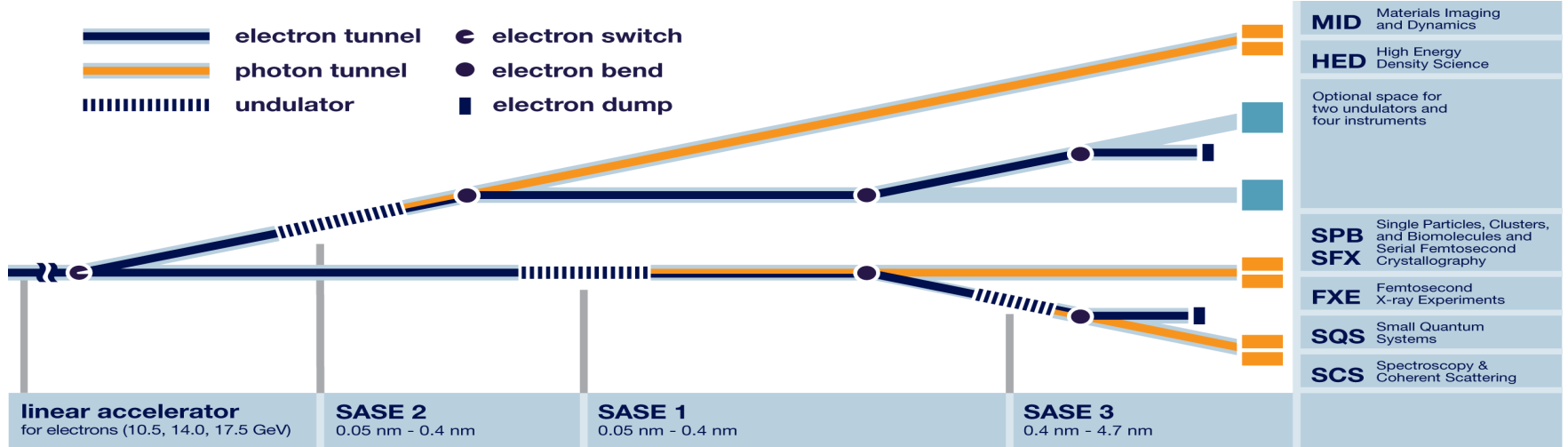
A. Marinelli et al., "High-intensity double-pulse X-ray free-electron laser." Nature Communications, 2015. DOI: 10.1038/ncomms7369



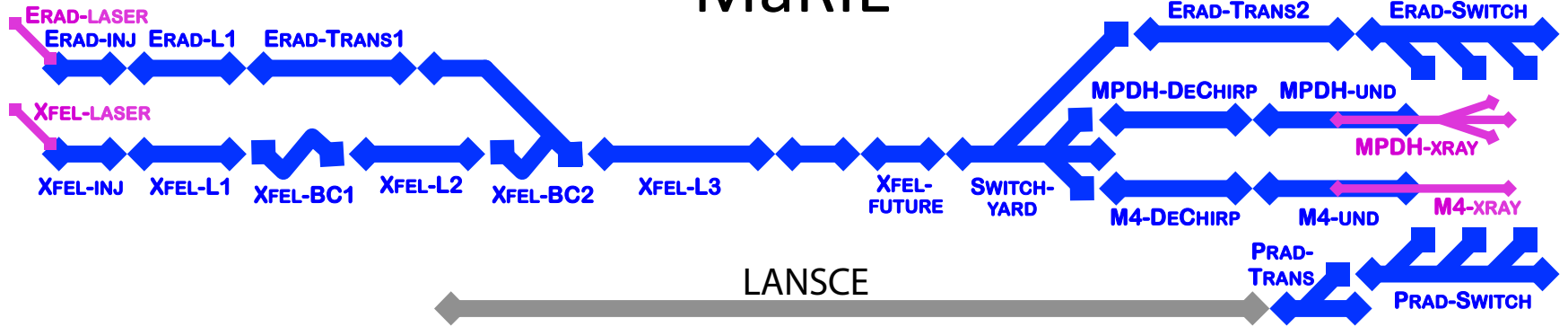
LCLS-II



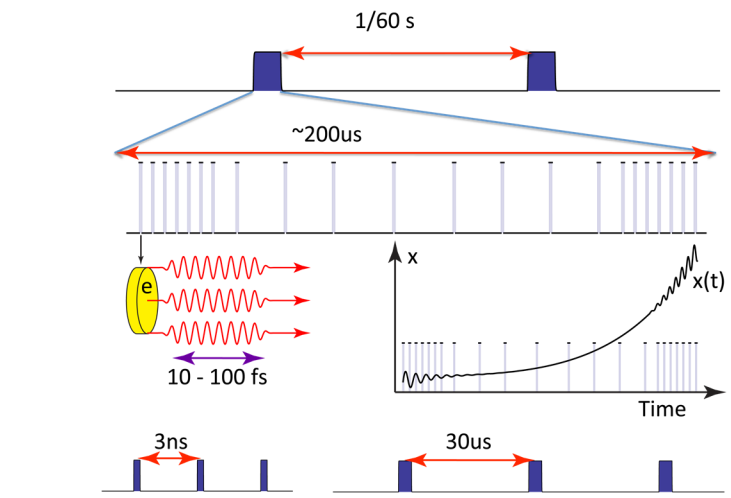
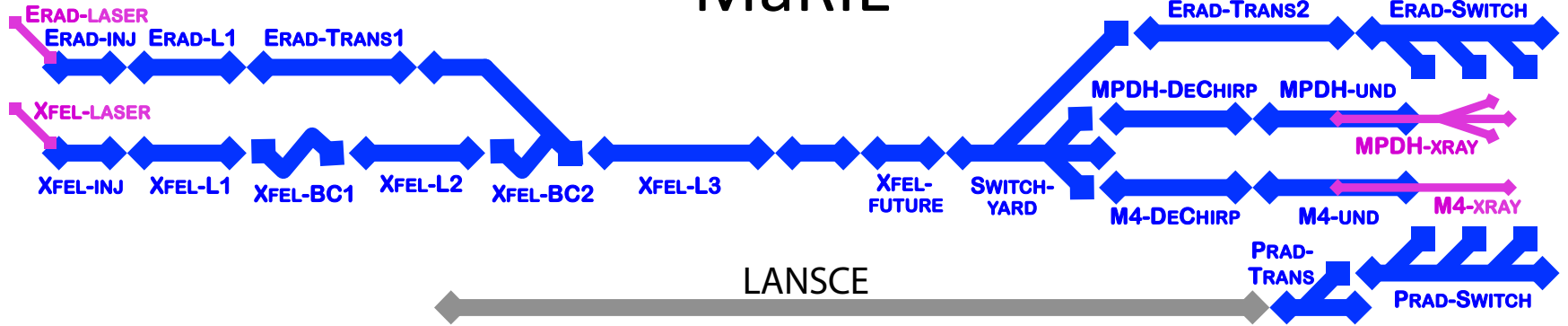
European XFEL



MaRIE



MaRIE



Photon energy: 4– 42 keV

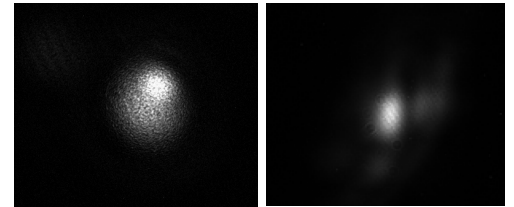
Accelerator Tuning Challenges

- Dynamics of intense charged particle bunches dominated by:
 - **Components drift unpredictably with time, misalignments**

Accelerator Tuning Challenges

- Dynamics of intense charged particle bunches dominated by:
 - Components drift unpredictably with time, misalignments
 - **Uncertain and time varying electron bunch distribution off cathode**
 - Complex collective effects:

@ FAST

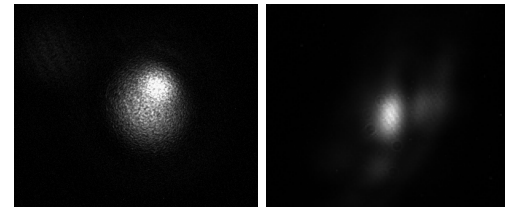


Example images of laser spot
(10 Aug. 2016, 11 Nov. 2017)

Accelerator Tuning Challenges

- Dynamics of intense charged particle bunches dominated by:
 - Components drift unpredictably with time, misalignments
 - **Uncertain and time varying electron bunch distribution off cathode**
 - **Complex collective effects:**
 - **Wakefields**
 - **Space charge**
 - **Coherent synchrotron radiation**

@ FAST

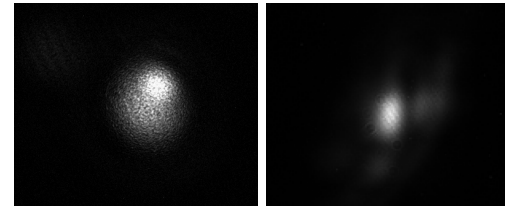


*Example images of laser spot
(10 Aug. 2016, 11 Nov. 2017)*

Accelerator Tuning Challenges

- Dynamics of intense charged particle bunches dominated by:
 - **Components drift unpredictably with time, misalignments**
 - **Uncertain and time varying electron bunch distribution off cathode**
 - **Complex collective effects:**
 - **Wakefields**
 - **Space charge**
 - **Coherent synchrotron radiation**
 - **Limited diagnostics**

@ FAST

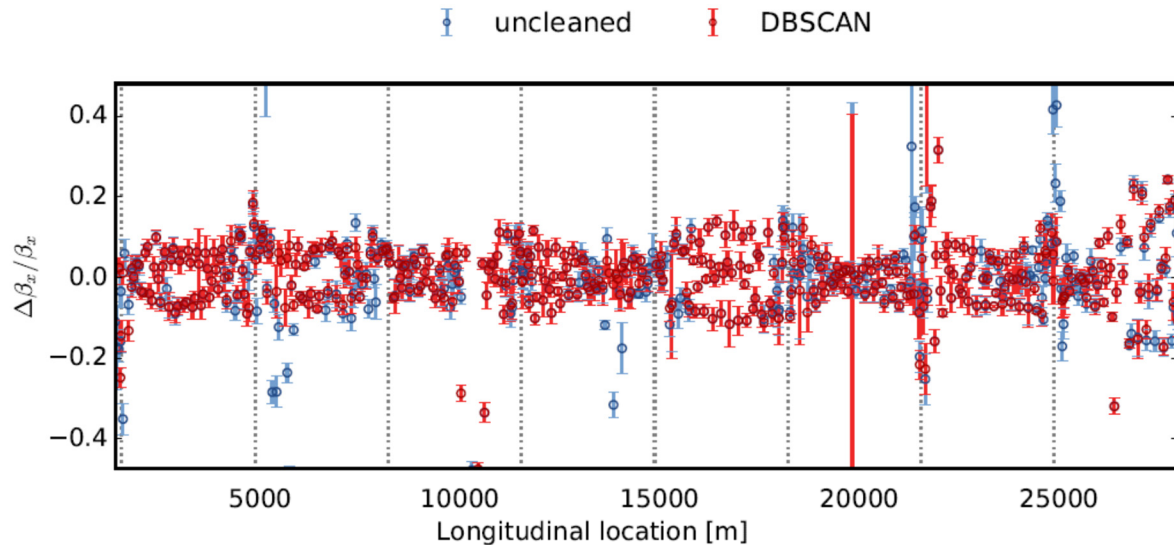
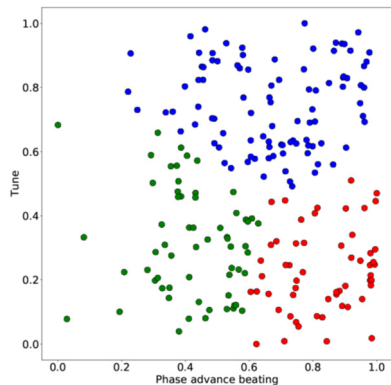
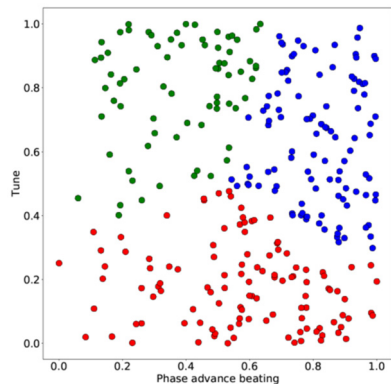


Example images of laser spot
(10 Aug. 2016, 11 Nov. 2017)

Machine Learning Approaches

ML for improvement of diagnostics

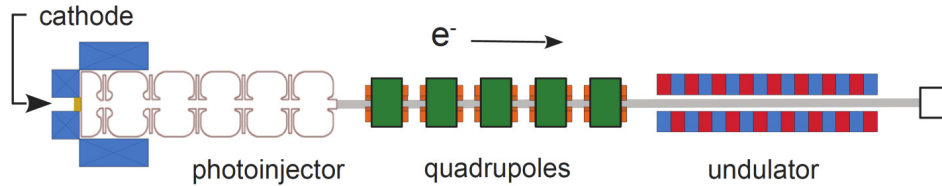
Detection of faulty BPMs at CERN (1024 BPMs) > Cluster analysis, faulty signals should appear as outliers



E. Fol and Tomas Garcia, Detection of faulty Beam Position Monitors at CERN
Machine Learning Applications for Particle Accelerators, Feb. 28 – March 2, 2018,
SLAC National Accelerator Laboratory

NN-based model for automatic FEL tuning

Compact, THz FEL design based on previously operational TEU-FEL



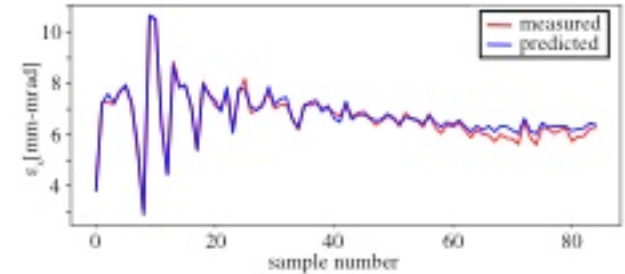
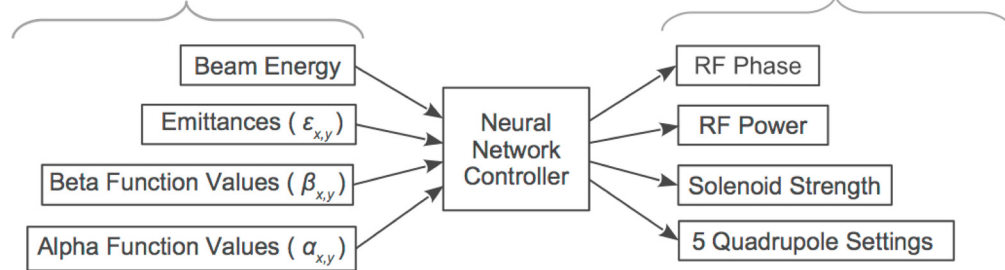
3 – 6 MeV electron beam
200 – 800 μm photon beam

Previously operated at University of Twente in the Netherlands

Was going to be re-built at CSU:
have simulation from design studies

desired electron beam characteristics at the entrance of the undulator

suggested machine settings to obtain the requested electron beam characteristics



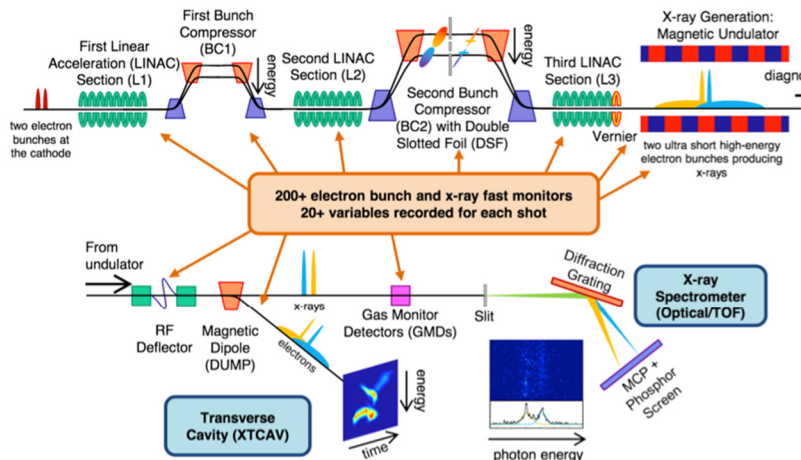
ML methods for shot-to-shot spectral profiling of FEL light

Machine learning applied to single-shot x-ray diagnostics in an XFEL

A. Sanchez-Gonzalez,¹ P. Micaelli,¹ C. Olivier,¹ T. R. Barillot,¹ M. Ilchen,^{2,3} A. A. Lutman,⁴ A. Marinelli,⁴ T. Maxwell,⁴ A. Achner,³ M. Agåker,⁵ N. Berrah,⁶ C. Bostedt,^{4,7} J. Buck,⁸ P. H. Bucksbaum,^{2,9} S. Carron Montero,^{4,10} B. Cooper,¹ J. P. Cryan,² M. Dong,⁵ R. Feifel,¹¹ L. J. Frasinski,¹ H. Fukuzawa,¹² A. Galler,³ G. Hartmann,^{8,13} N. Hartmann,⁴ W. Helml,^{4,14} A. S. Johnson,¹ A. Knie,¹³ A. O. Lindahl,^{2,11} J. Liu,³ K. Motomura,¹² M. Mucke,⁵ C. O'Grady,⁴ J-E. Rubensson,⁵ E. R. Simpson,¹ R. J. Squibb,¹¹ C. Sätze,¹⁵ K. Ueda,¹² M. Vacher,^{16,17} D. J. Walke,¹ V. Zhaunerchyk,¹¹ R. N. Coffee,⁴ and J. P. Marangos¹

- Used archived data to learn correlation between fast and slow diagnostics

Shot-to-shot data: Current profiles, BPMs, X-ray gas detectors



A. Sanchez-Gonzalez, et al. <https://arxiv.org/pdf/1610.03378.pdf>

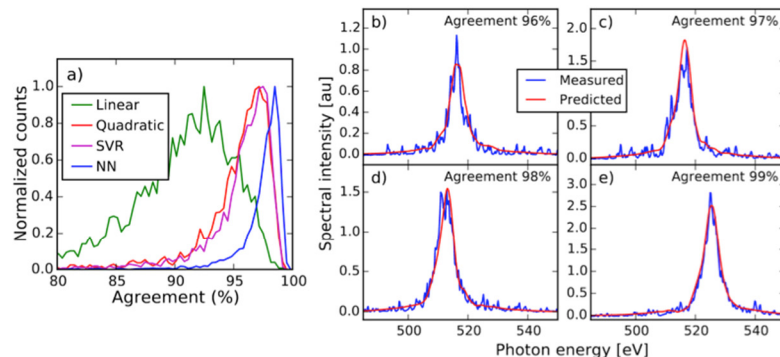
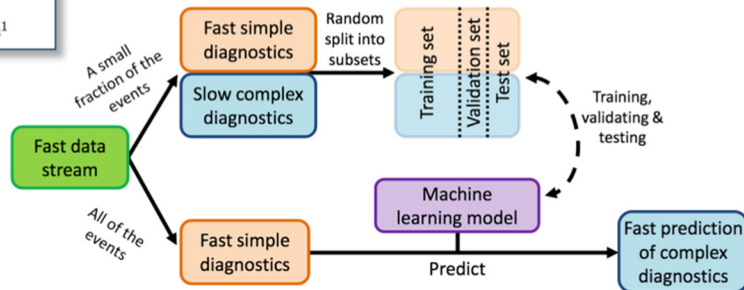


FIG. 4. Spectral shape prediction for a single pulse. (a) Histogram of agreements between the predicted and the measured spectra for the test set using the 4 different models. (b-e) Examples of the measured and the predicted spectra using a neural network to illustrate the accuracy for different agreement values.

Machine Learning Approaches
(mostly statistics and big data so far)

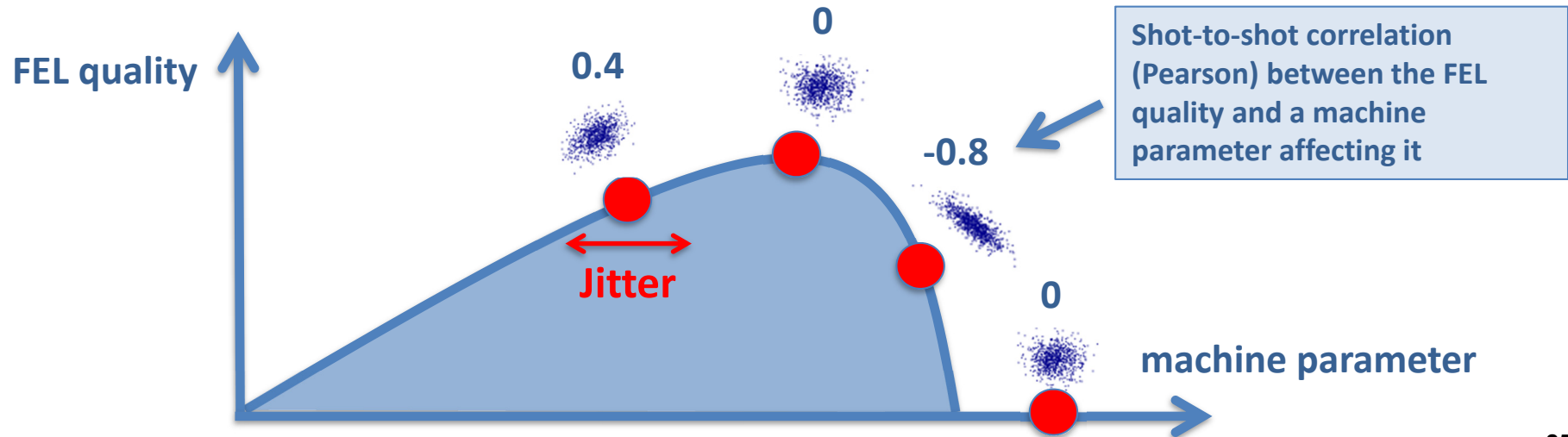
Machine Learning Approaches
(mostly statistics and big data so far)

**Automatic Feedback for in-hardware Tuning
and Optimization**

FERMI: Optimization Through Correlation Minimization

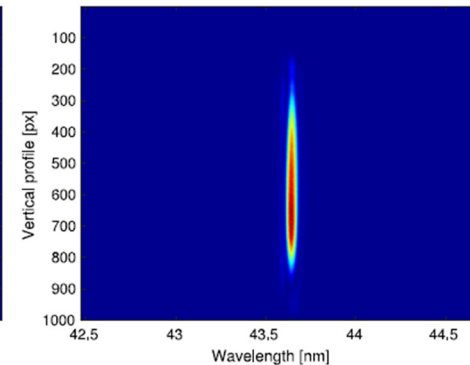
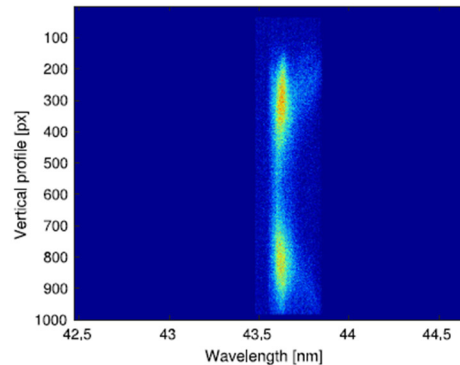
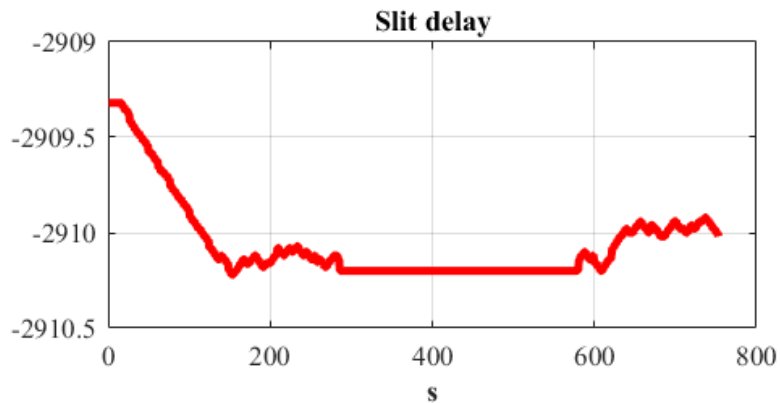
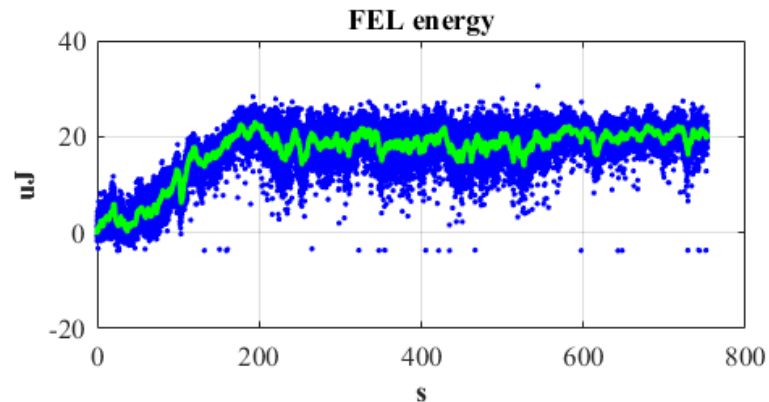
- Giulio Gaio, IFCA Machine Learning Workshop, SLAC, 03/02/2018

- Automatic optimization of the temporal overlap between seed laser pulse and electron bunch (1 variable)
- Correlation between the electron bunch arrival time (*sensor*) and the FEL energy (*target*)
- The actuator is a mechanical delay line (slit) on the seed laser path



FERMI: Optimization Through Correlation Minimization

- Giulio Gaio, IFCA Machine Learning Workshop, SLAC, 03/02/2018



The **FEL Quality Factor** (*FELQFactor*): index which summarizing, in a number, the **most important features of the photon energy spectrum**: intensity, spectral purity and number of modes.

Actuator: seed laser delay line.

“Free-electron Laser Spectrum Evaluation and Automatic Optimization”,
Nuclear Inst. and Methods in Physics Research, A 871 (2017) 20 29

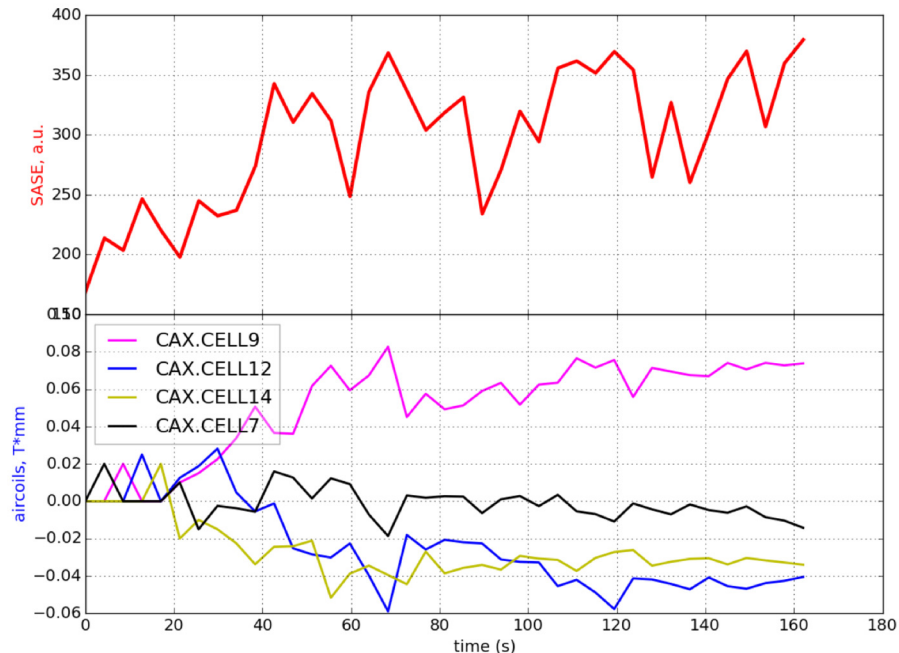
OCELT at EUXFEL

Generic optimizer: SASE optimization

- Air coils between the undulator cells were used to optimize the SASE signal
- Up to 6 air coils are typically used at the same time.

Nelder-Mead (simplex) and conjugate gradient (CG) method

- Limited to ~6 parameters
- Won't work with large hysteresis
- Won't work with time-varying system



Tuning Method Currently Being Developed at LANL

Extremum Seeking

Model-independent feedback

- Noisy and time varying systems
- Many coupled parameters

Bounded Extremum Seeking: Model-Independent Tuning and Optimization

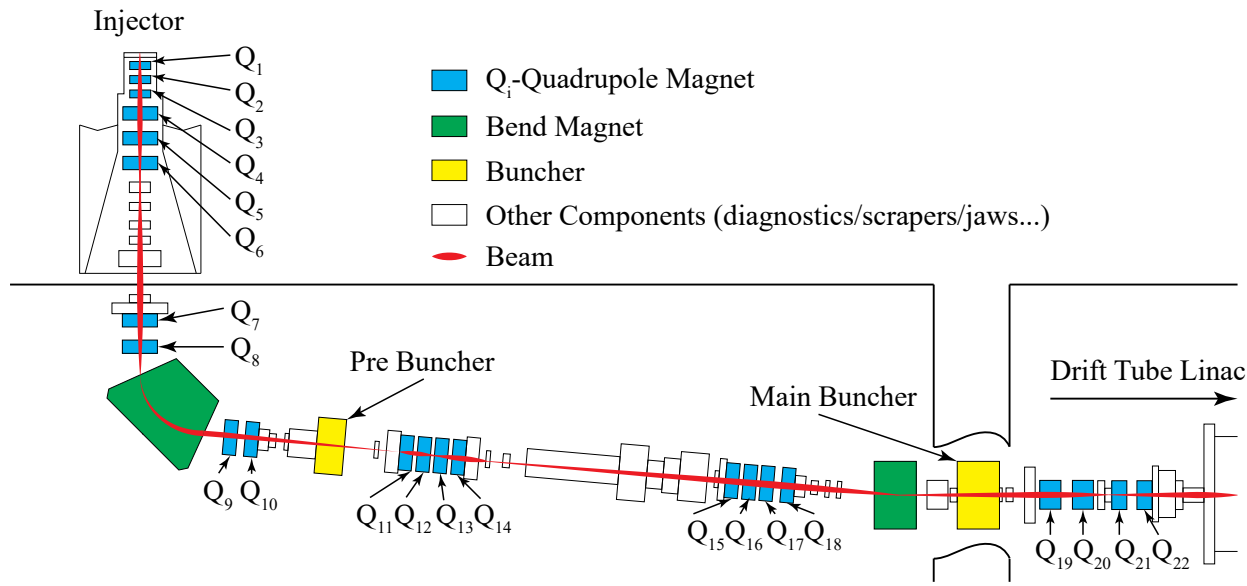
A. Scheinker and D. Scheinker, "Extremum Seeking with Discontinuous Dithers," *Automatica*, vol. 69, pp. 250-257, 2016.

A. Scheinker and D. Scheinker, "Extremum Seeking for Stabilization of Systems not Affine in Control," 2017.

$$\begin{bmatrix} \dot{x}_1 \\ \vdots \\ \dot{x}_n \end{bmatrix} = \dot{\mathbf{x}} = \mathbf{f}(\mathbf{x}, \mathbf{p}, t) = \begin{bmatrix} f_1(x_1, \dots, x_n, p_1, \dots, p_m, t) \\ \vdots \\ f_n(x_1, \dots, x_n, p_1, \dots, p_m, t) \end{bmatrix}$$

Bounded Extremum Seeking: Model-Independent Tuning and Optimization

$$\begin{bmatrix} \dot{x}_1 \\ \vdots \\ \dot{x}_n \end{bmatrix} = \dot{\mathbf{x}} = \mathbf{f}(\mathbf{x}, \mathbf{p}, t) = \begin{bmatrix} f_1(x_1, \dots, x_n, p_1, \dots, p_m, t) \\ \vdots \\ f_n(x_1, \dots, x_n, p_1, \dots, p_m, t) \end{bmatrix}$$



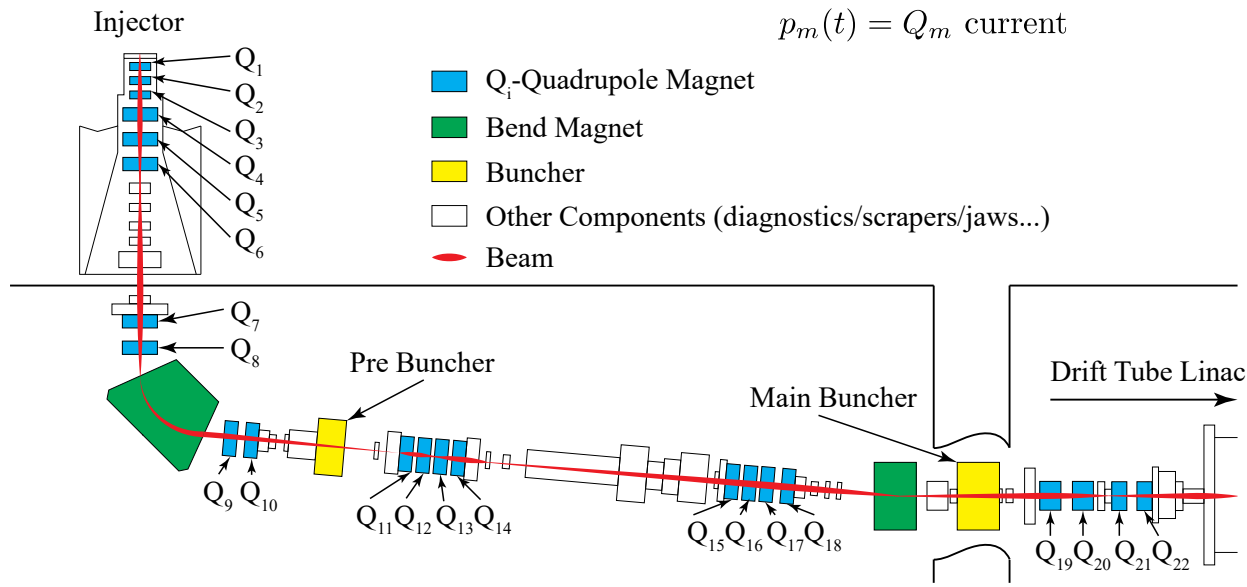
Bounded Extremum Seeking: Model-Independent Tuning and Optimization

$$\begin{bmatrix} \dot{x}_1 \\ \vdots \\ \dot{x}_n \end{bmatrix} = \dot{\mathbf{x}} = \mathbf{f}(\mathbf{x}, \mathbf{p}, t) = \begin{bmatrix} f_1(x_1, \dots, x_n, p_1, \dots, p_m, t) \\ \vdots \\ f_n(x_1, \dots, x_n, p_1, \dots, p_m, t) \end{bmatrix}$$

$p_1(t) = Q_1$ current

\vdots

$p_m(t) = Q_m$ current



Bounded Extremum Seeking: Model-Independent Tuning and Optimization

$$\begin{bmatrix} \dot{x}_1 \\ \vdots \\ \dot{x}_n \end{bmatrix} = \dot{\mathbf{x}} = \mathbf{f}(\mathbf{x}, \mathbf{p}, t) = \begin{bmatrix} f_1(x_1, \dots, x_n, p_1, \dots, p_m, t) \\ \vdots \\ f_n(x_1, \dots, x_n, p_1, \dots, p_m, t) \end{bmatrix}$$

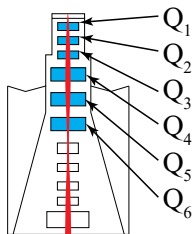
$$p_1(t) = Q_1 \text{ current} \quad x_1(t) = X_{\text{rms}}(\text{position 1})$$

$$\vdots \quad x_2(t) = Y_{\text{rms}}(\text{position 1})$$

$$p_m(t) = Q_m \text{ current} \quad \vdots$$

$$x_n(t) = X_{\text{rms}}(\text{position n})$$

Injector



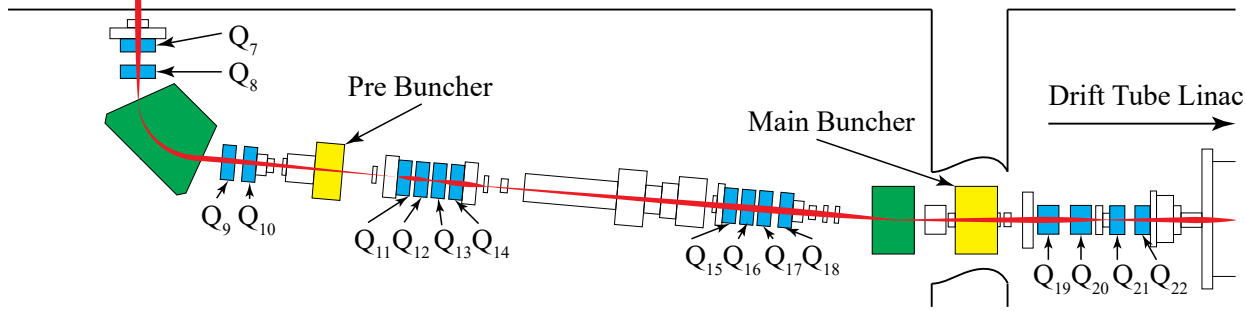
■ Q_i -Quadrupole Magnet

■ Bend Magnet

■ Buncher

Other Components (diagnostics/scrapers/jaws...)

— Beam



Bounded Extremum Seeking: Model-Independent Tuning and Optimization

$$\begin{bmatrix} \dot{x}_1 \\ \vdots \\ \dot{x}_n \end{bmatrix} = \dot{\mathbf{x}} = \mathbf{f}(\mathbf{x}, \mathbf{p}, t) = \begin{bmatrix} f_1(x_1, \dots, x_n, p_1, \dots, p_m, t) \\ \vdots \\ f_n(x_1, \dots, x_n, p_1, \dots, p_m, t) \end{bmatrix}$$

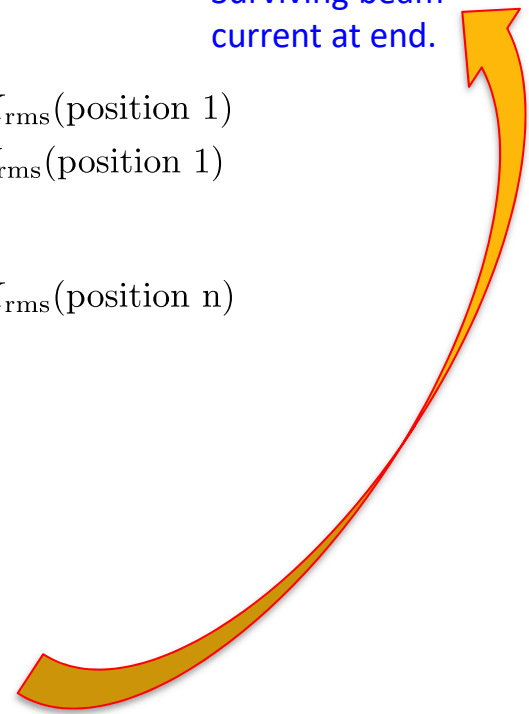
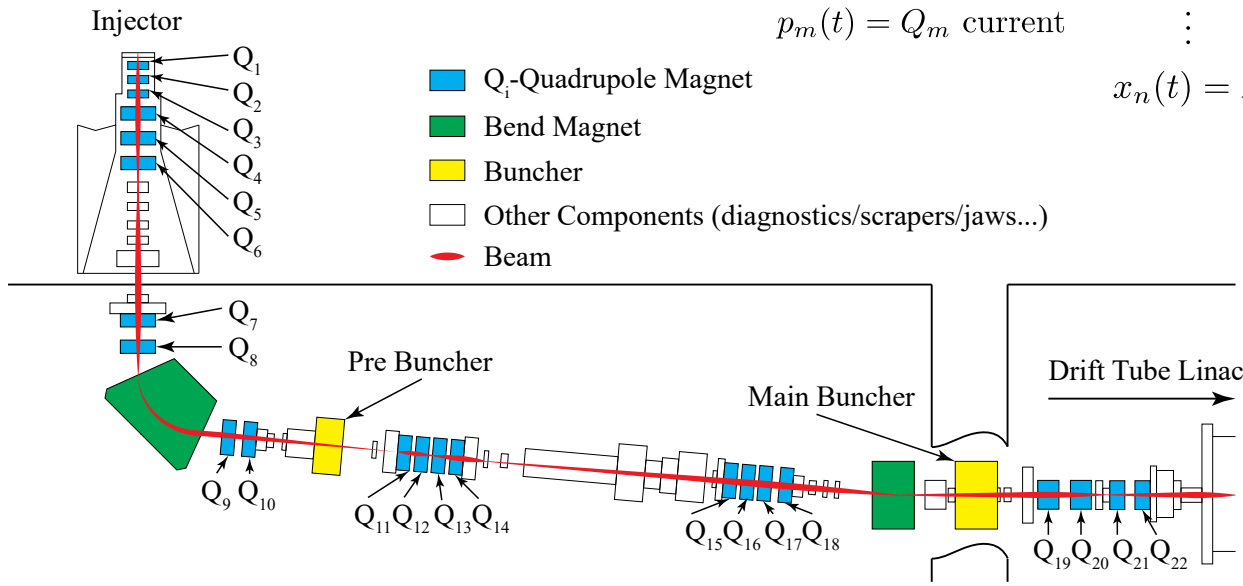
$$y = V(\mathbf{x}, t) + n(t)$$

noise

$$y = (I(t) - I_0)^2 + n(t)$$

Surviving beam
current at end.

$$\begin{array}{ll} p_1(t) = Q_1 \text{ current} & x_1(t) = X_{\text{rms}}(\text{position 1}) \\ \vdots & x_2(t) = Y_{\text{rms}}(\text{position 1}) \\ p_m(t) = Q_m \text{ current} & \vdots \\ & x_n(t) = X_{\text{rms}}(\text{position n}) \end{array}$$



$$\begin{bmatrix} \dot{x}_1 \\ \vdots \\ \dot{x}_n \end{bmatrix} = \dot{\mathbf{x}} = \mathbf{f}(\mathbf{x}, \mathbf{p}, t) = \begin{bmatrix} f_1(x_1, \dots, x_n, p_1, \dots, p_m, t) \\ \vdots \\ f_n(x_1, \dots, x_n, p_1, \dots, p_m, t) \end{bmatrix}$$

$$y = V(\mathbf{x}, t) + n(t)$$

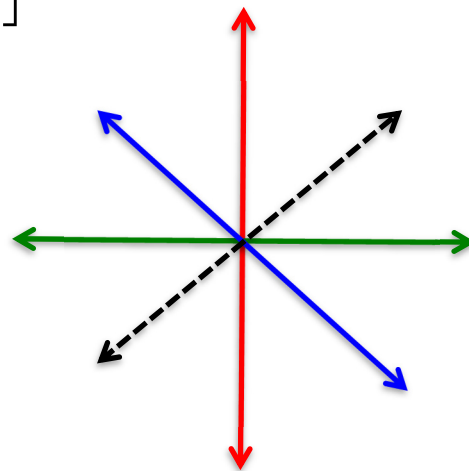
$$\frac{dp_1}{dt} = \sqrt{\alpha\omega_1} \cos(\omega_1 t + ky)$$

$$\frac{dp_2}{dt} = \sqrt{\alpha\omega_2} \cos(\omega_2 t + ky)$$

$$\frac{dp_3}{dt} = \sqrt{\alpha\omega_3} \cos(\omega_3 t + ky)$$

$$\vdots$$

$$\frac{dp_m}{dt} = \sqrt{\alpha\omega_m} \cos(\omega_m t + ky)$$



Dithering with different frequencies makes the parameters “perpendicular” in Hilbert space.

$$\omega_i = \omega r_i, \quad r_i \neq r_j \implies \text{for any } t > 0$$

$$\lim_{\omega \rightarrow \infty} \langle \cos(\omega_i t), \cos(\omega_j t) \rangle = \lim_{\omega \rightarrow \infty} \int_0^t \cos(\omega_i \tau) \cos(\omega_j \tau) d\tau = 0$$

$$\begin{bmatrix} \dot{x}_1 \\ \vdots \\ \dot{x}_n \end{bmatrix} = \dot{\mathbf{x}} = \mathbf{f}(\mathbf{x}, \mathbf{p}, t) = \begin{bmatrix} f_1(x_1, \dots, x_n, p_1, \dots, p_m, t) \\ \vdots \\ f_n(x_1, \dots, x_n, p_1, \dots, p_m, t) \end{bmatrix}$$

$$y = V(\mathbf{x}, t) + n(t)$$

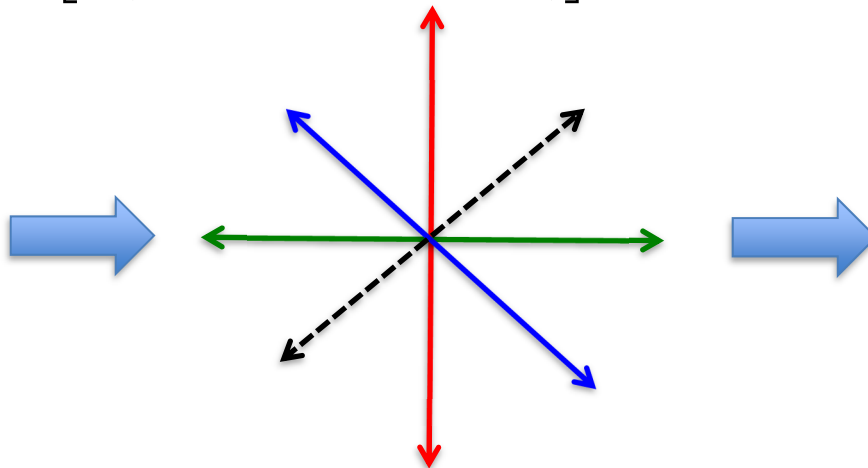
$$\frac{dp_1}{dt} = \sqrt{\alpha\omega_1} \cos(\omega_1 t + ky)$$

$$\frac{dp_2}{dt} = \sqrt{\alpha\omega_2} \cos(\omega_2 t + ky)$$

$$\frac{dp_3}{dt} = \sqrt{\alpha\omega_3} \cos(\omega_3 t + ky)$$

⋮

$$\frac{dp_m}{dt} = \sqrt{\alpha\omega_m} \cos(\omega_m t + ky)$$



Allows simultaneous tuning of ALL parameters in parallel.

$$\frac{d\mathbf{p}}{dt} = -\frac{k\alpha}{2} (\nabla_{\mathbf{p}} V(\mathbf{x}, t))^T$$

On average, the system performs minimizes the **unknown, time-varying** function $V(\mathbf{x}, t)$

$$\omega_i = \omega r_i, \quad r_i \neq r_j \implies \text{for any } t > 0$$

$$\lim_{\omega \rightarrow \infty} \langle \cos(\omega_i t), \cos(\omega_j t) \rangle = \lim_{\omega \rightarrow \infty} \int_0^t \cos(\omega_i \tau) \cos(\omega_j \tau) d\tau = 0$$

Bounded Extremum Seeking: Model-Independent Tuning and Optimization

$$\begin{bmatrix} \dot{x}_1 \\ \vdots \\ \dot{x}_n \end{bmatrix} = \dot{\mathbf{x}} = \mathbf{f}(\mathbf{x}, \mathbf{p}, t) = \begin{bmatrix} f_1(x_1, \dots, x_n, p_1, \dots, p_m, t) \\ \vdots \\ f_n(x_1, \dots, x_n, p_1, \dots, p_m, t) \end{bmatrix}$$

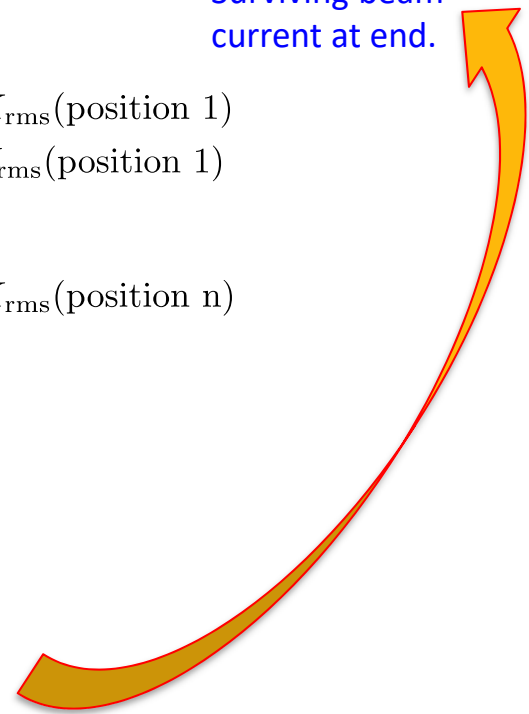
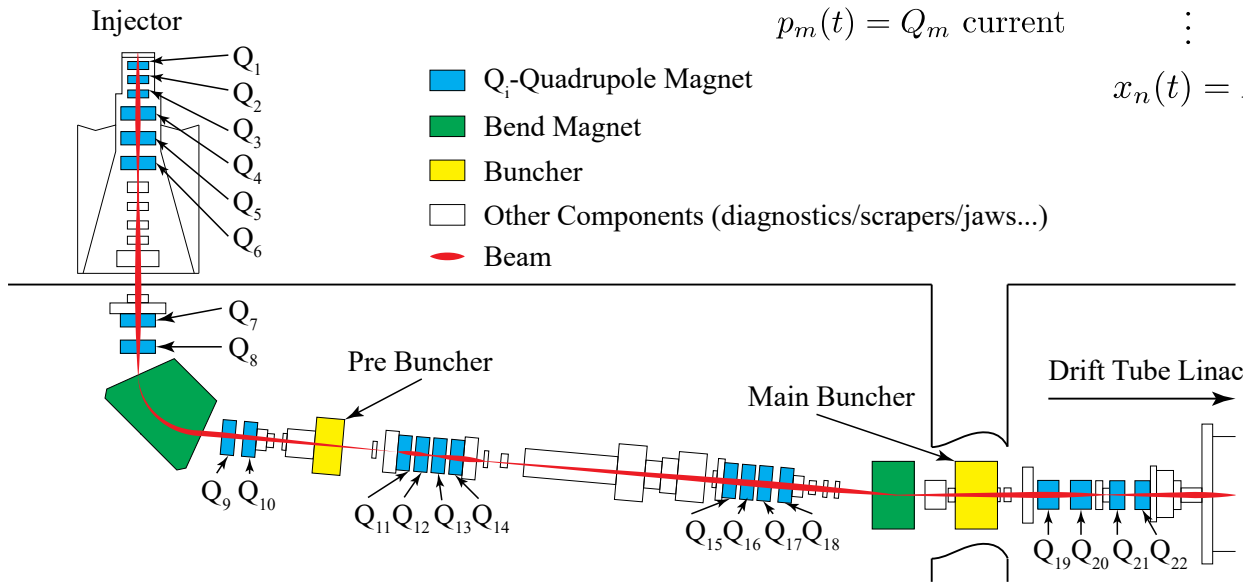
$$y = V(\mathbf{x}, t) + n(t)$$

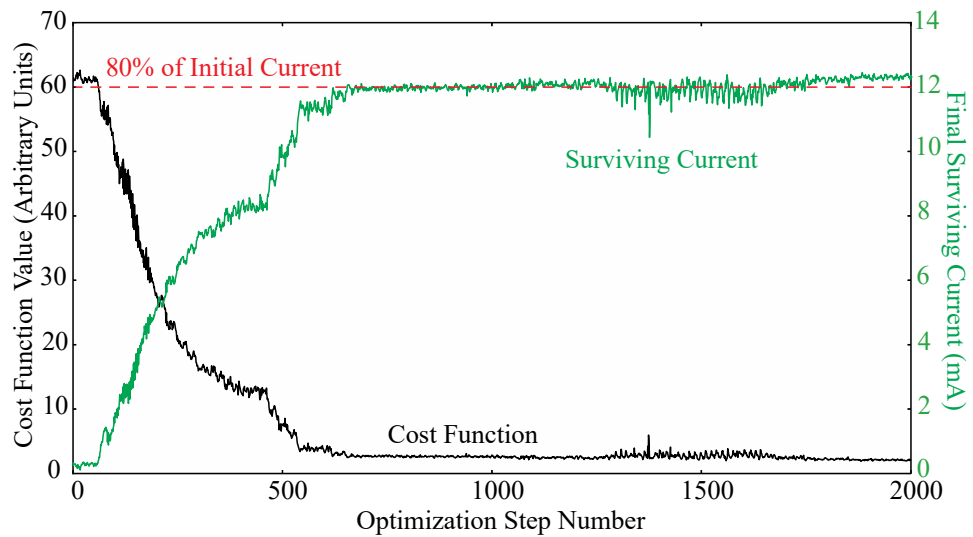
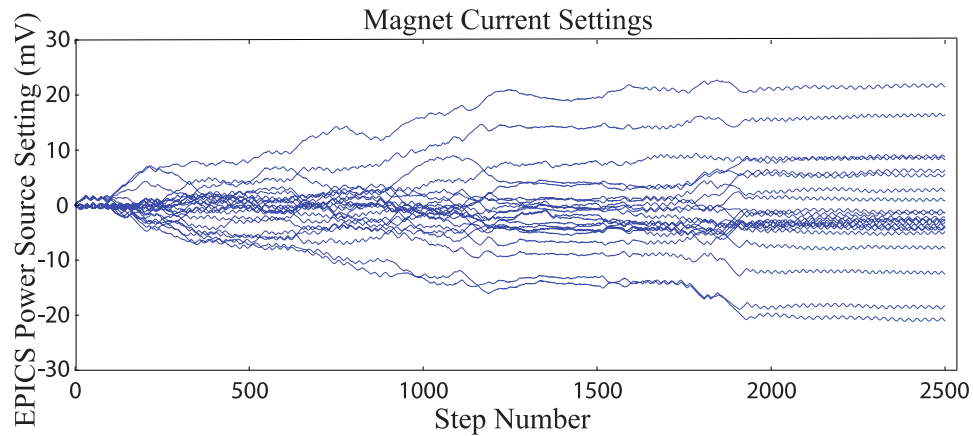
noise

$$y = (I(t) - I_0)^2 + n(t)$$

Surviving beam
current at end.

$$\begin{array}{ll} p_1(t) = Q_1 \text{ current} & x_1(t) = X_{\text{rms}}(\text{position 1}) \\ \vdots & x_2(t) = Y_{\text{rms}}(\text{position 1}) \\ p_m(t) = Q_m \text{ current} & \vdots \\ & x_n(t) = X_{\text{rms}}(\text{position n}) \end{array}$$





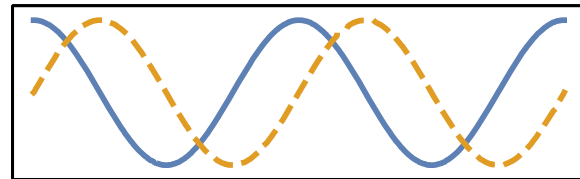
$$\dot{x} = x + 0.5y + u_x$$

$$\dot{y} = 0.75x + 2y + u_y$$

$$h = x^2 + y^2$$

$$u_{1,x} = \cos(\omega t + kh(x, y))\sqrt{\alpha\omega}$$

$$u_{1,y} = \sin(\omega t + kh(x, y))\sqrt{\alpha\omega}$$



$$\dot{x} = x + 0.5y + u_x$$

$$\dot{y} = 0.75x + 2y + u_y$$

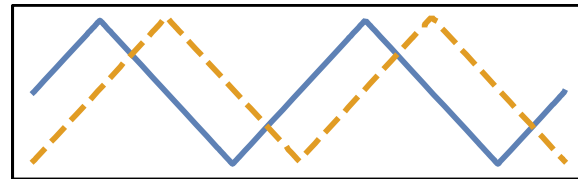
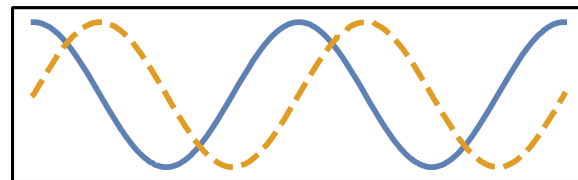
$$h = x^2 + y^2$$

$$u_{1,x} = \cos(\omega t + kh(x, y))\sqrt{\alpha\omega}$$

$$u_{1,y} = \sin(\omega t + kh(x, y))\sqrt{\alpha\omega}$$

$$u_{2,x} = f_{\text{tri},1}(\omega t + kh(x, y))\frac{4}{\pi}\sqrt{\alpha\omega}$$

$$u_{2,y} = f_{\text{tri},2}(\omega t + kh(x, y))\frac{4}{\pi}\sqrt{\alpha\omega}$$



$$\dot{x} = x + 0.5y + u_x$$

$$\dot{y} = 0.75x + 2y + u_y$$

$$h = x^2 + y^2$$

$$u_{1,x} = \cos(\omega t + kh(x, y))\sqrt{\alpha\omega}$$

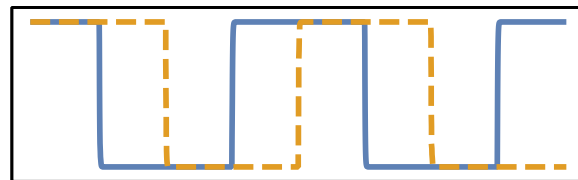
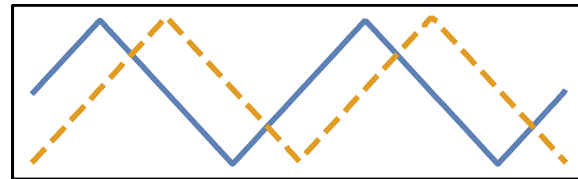
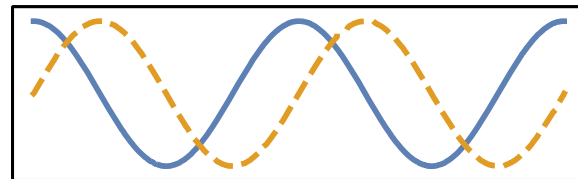
$$u_{1,y} = \sin(\omega t + kh(x, y))\sqrt{\alpha\omega}$$

$$u_{2,x} = f_{\text{tri},1}(\omega t + kh(x, y))\frac{4}{\pi}\sqrt{\alpha\omega}$$

$$u_{2,y} = f_{\text{tri},2}(\omega t + kh(x, y))\frac{4}{\pi}\sqrt{\alpha\omega}$$

$$u_{3,x} = f_{\text{sqr},1}(\omega t + kh(x, y))\frac{2}{\pi}\sqrt{\alpha\omega}$$

$$u_{3,y} = f_{\text{sqr},2}(\omega t + kh(x, y))\frac{2}{\pi}\sqrt{\alpha\omega}$$



$$\dot{x} = x + 0.5y + u_x$$

$$\dot{y} = 0.75x + 2y + u_y$$

$$h = x^2 + y^2$$

$$u_{1,x} = \cos(\omega t + kh(x, y))\sqrt{\alpha\omega}$$

$$u_{1,y} = \sin(\omega t + kh(x, y))\sqrt{\alpha\omega}$$

$$u_{2,x} = f_{\text{tri},1}(\omega t + kh(x, y))\frac{4}{\pi}\sqrt{\alpha\omega}$$

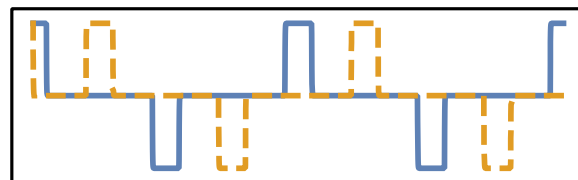
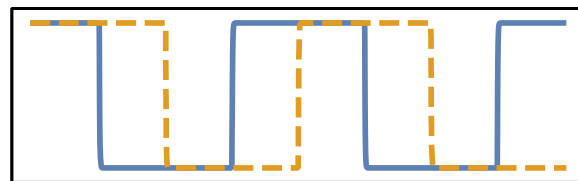
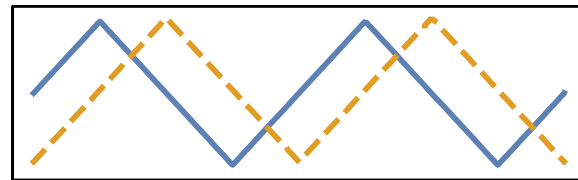
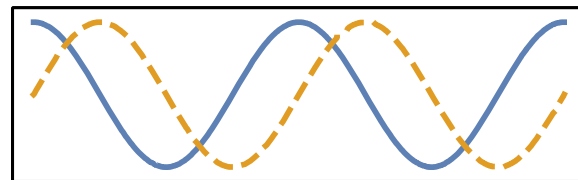
$$u_{2,y} = f_{\text{tri},2}(\omega t + kh(x, y))\frac{4}{\pi}\sqrt{\alpha\omega}$$

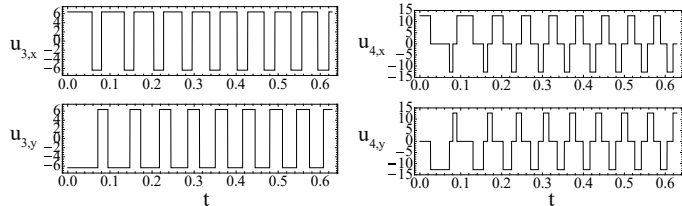
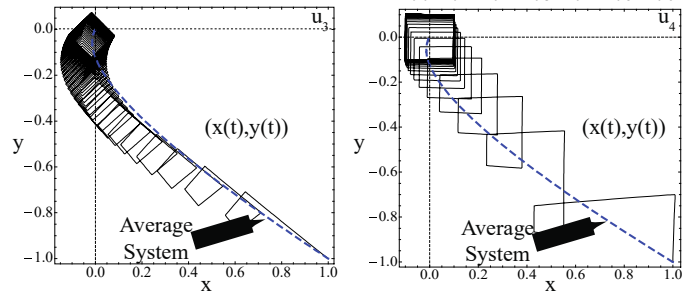
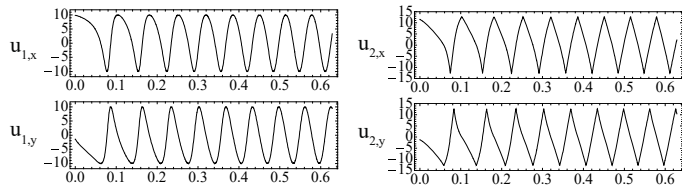
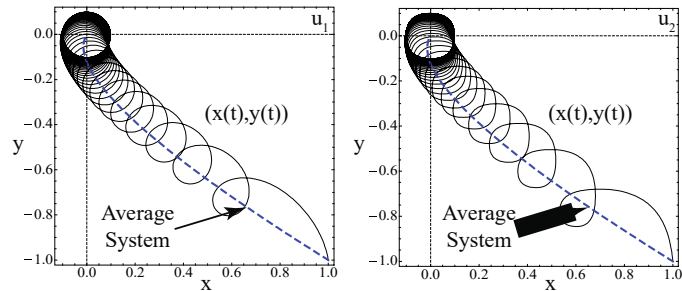
$$u_{3,x} = f_{\text{sqr},1}(\omega t + kh(x, y))\frac{2}{\pi}\sqrt{\alpha\omega}$$

$$u_{3,y} = f_{\text{sqr},2}(\omega t + kh(x, y))\frac{2}{\pi}\sqrt{\alpha\omega}$$

$$u_{4,x} = f_{\text{sqr},1}(\omega t + kh(x, y))\frac{2}{\pi}\sqrt{\alpha\omega}$$

$$u_{4,y} = f_{\text{sqr},2}(\omega t + kh(x, y))\frac{2}{\pi}\sqrt{\alpha\omega}$$

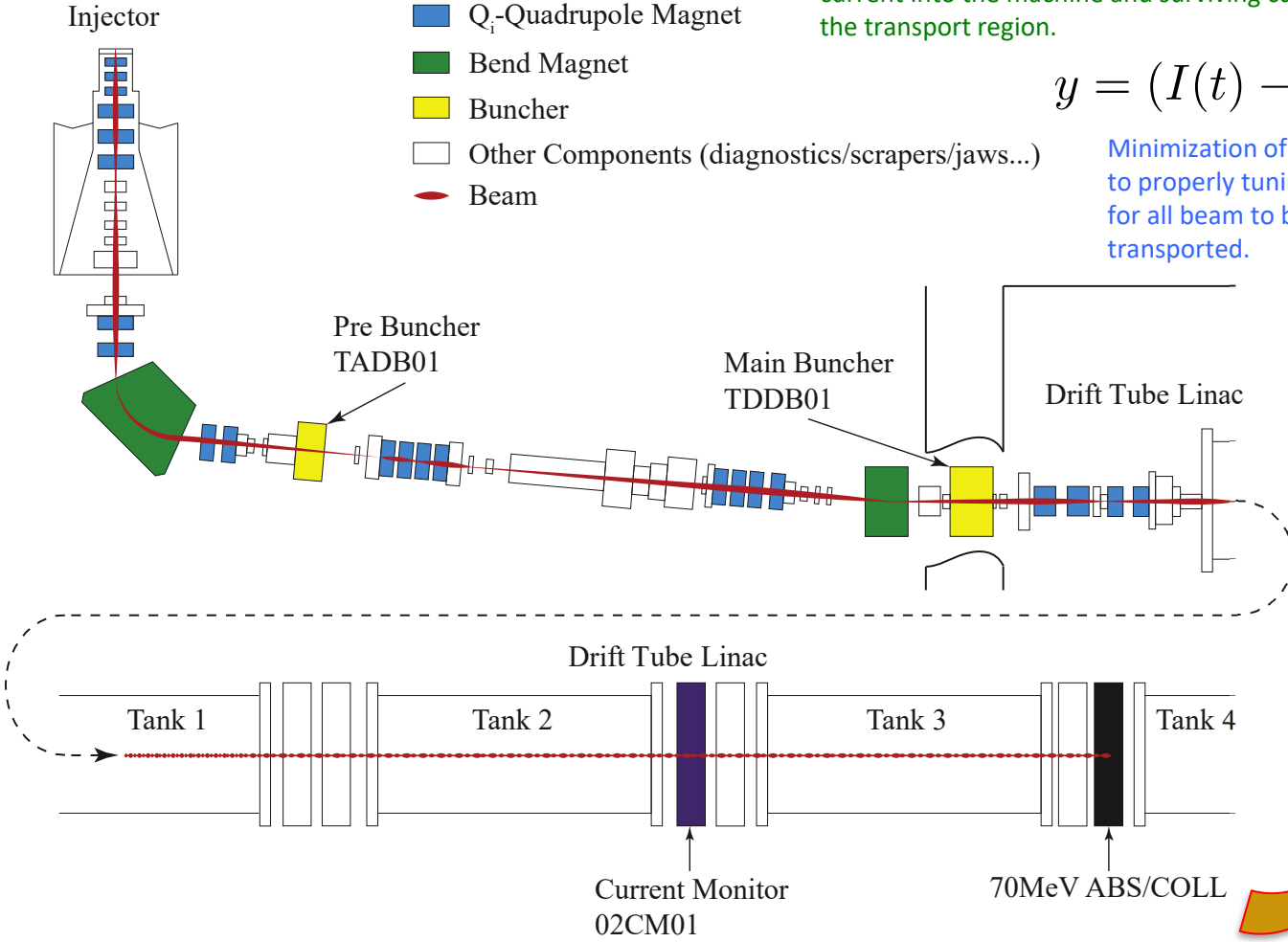




Cost is noisy measurement of the difference between initial current into the machine and surviving current at the end of the transport region.

$$y = (I(t) - I_0)^2 + n(t)$$

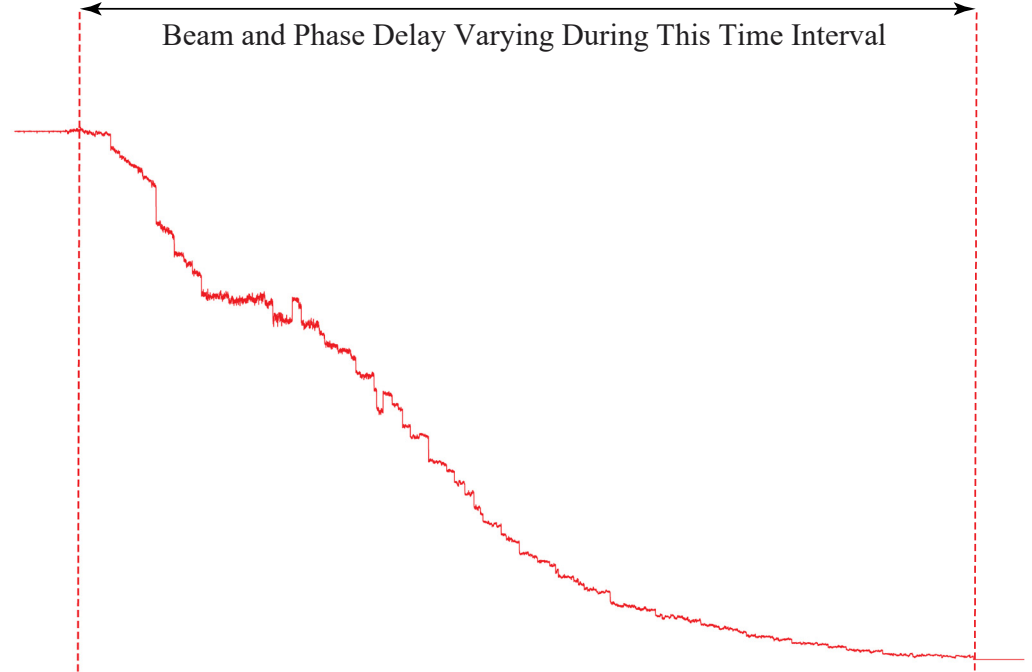
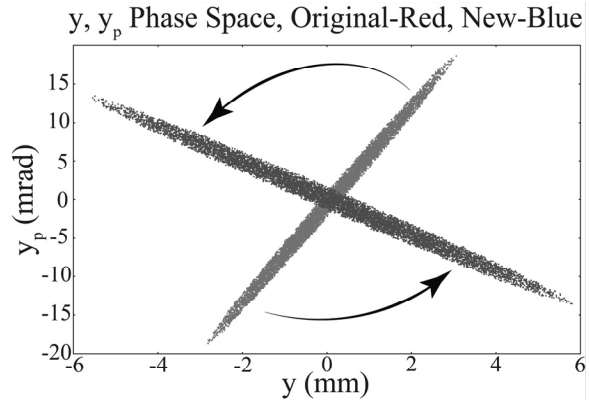
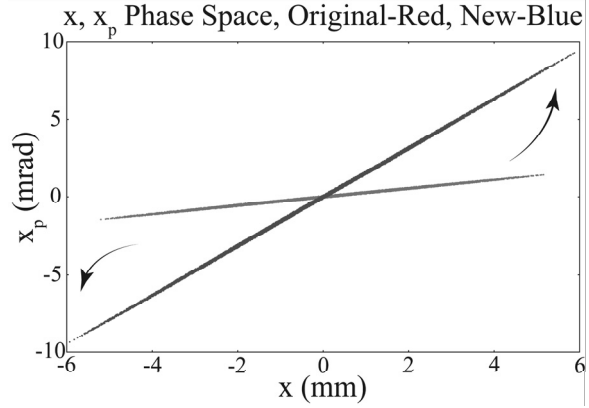
Minimization of y equivalent to properly tuning magnets for all beam to be transported.



After the magnetic lattice was matched to transport the beam, beam phase space was continuously varied, and arbitrary phase drifts were introduced into the RF buncher cavities.

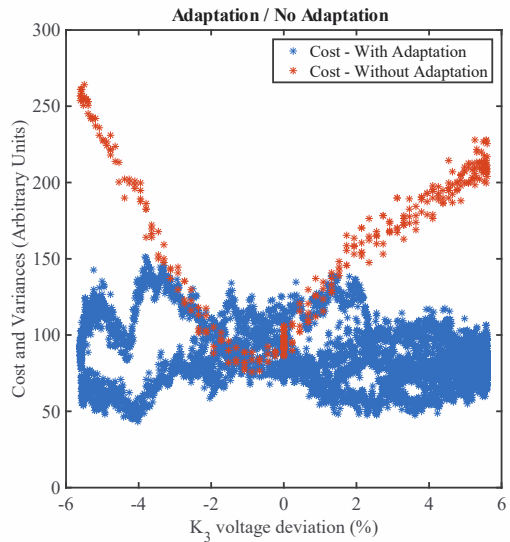
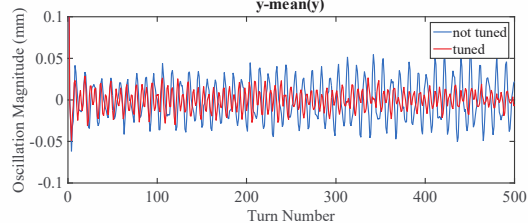
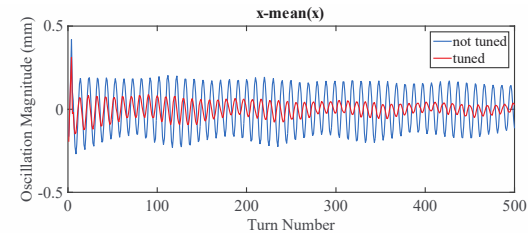
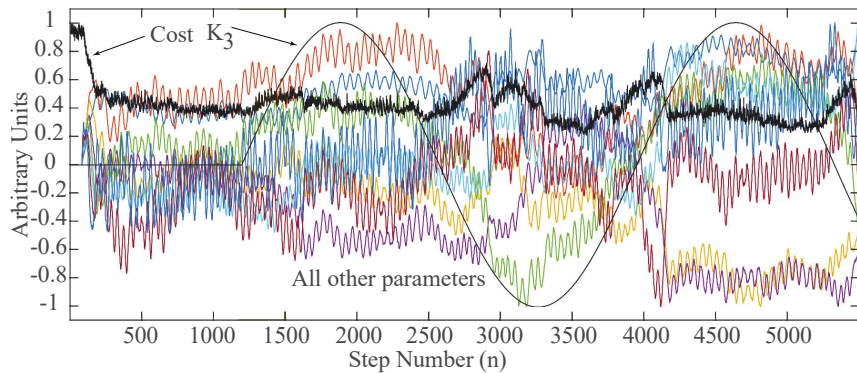
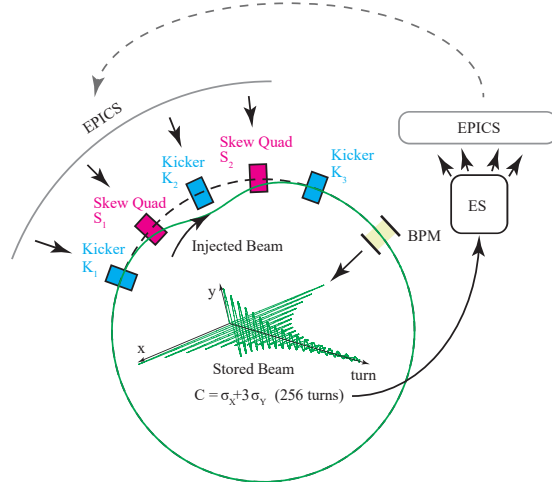
Without adaptive feedback all beam is quickly lost (red line in figure below).

With adaptive tuning the 22 quad magnetic lattice and 2 RF buncher cavities are continuously re-tuned to maintain maximal beam transmission and acceleration.

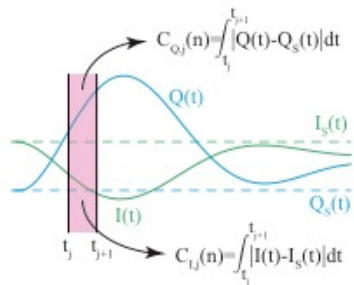


A. Scheinker et al., "Minimization of Betatron oscillations of electron beam injected into a time-varying lattice via extremum seeking," *IEEE Transactions on Control Systems Technology*, 2016.

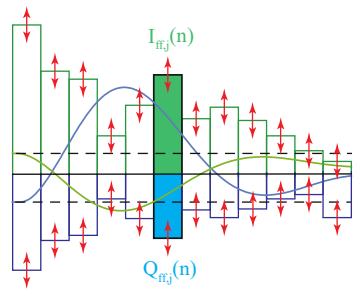
SPEAR3 time-varying magnetic lattice



A. Scheinker. "Iterative Extremum Seeking for Feedforward Compensation of Beam Loading in Particle Accelerator RF Cavities," in *Proceedings of the 2017 American Control Conference*, May, 2017.

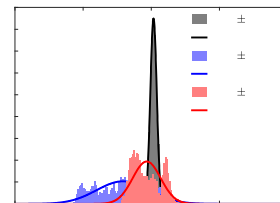
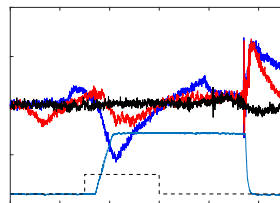
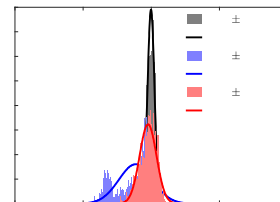
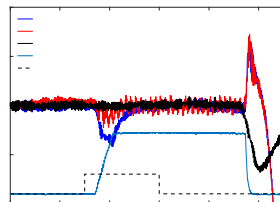
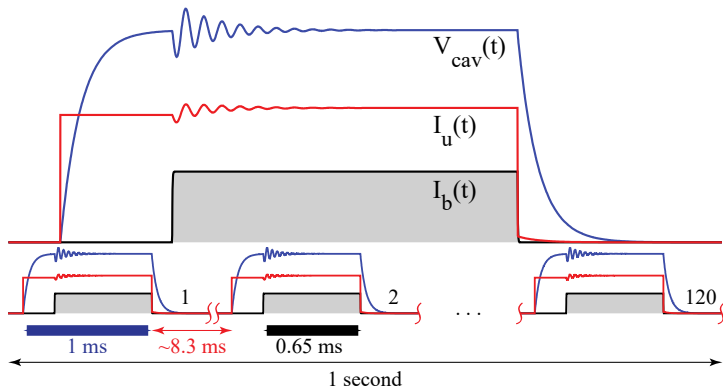


Break up cavity field errors into slices and create costs for iterative minimization

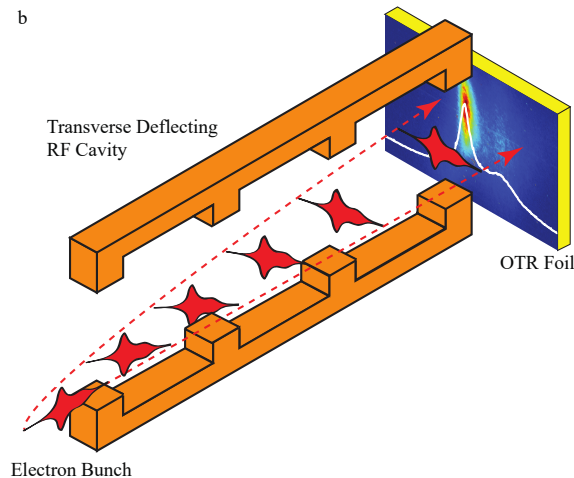
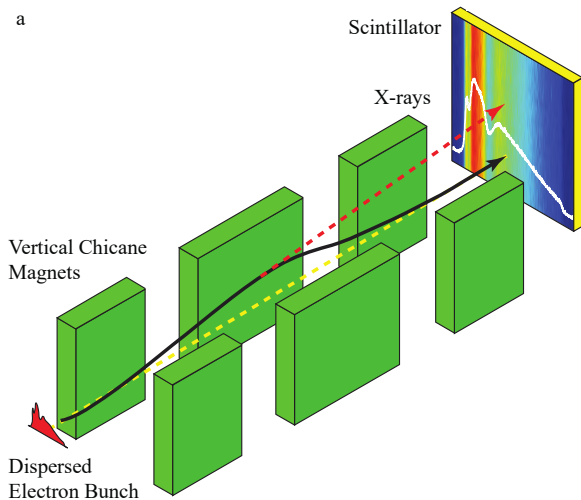
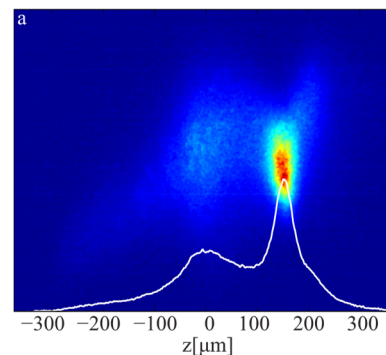
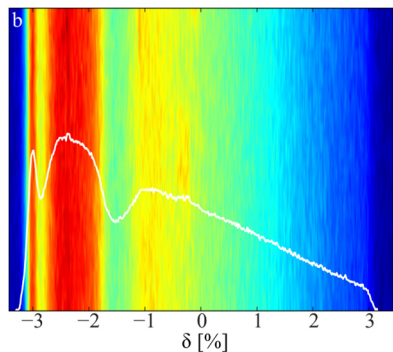


Create feed-forward waveforms for each slice to compensate for beam loading

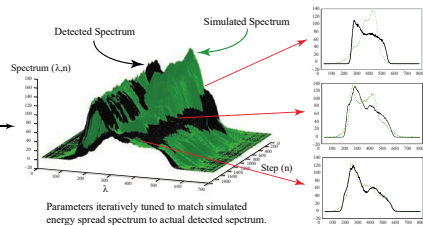
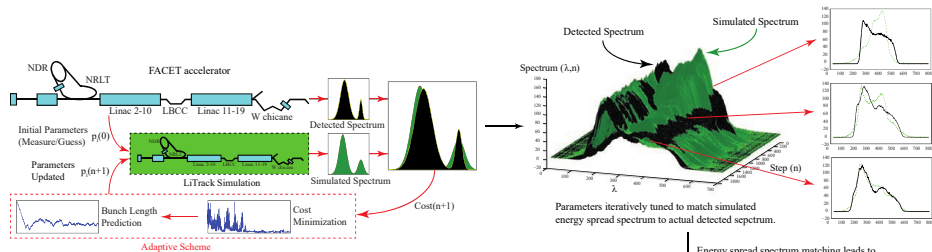
H+ 21mA peak current, 625μs pulses



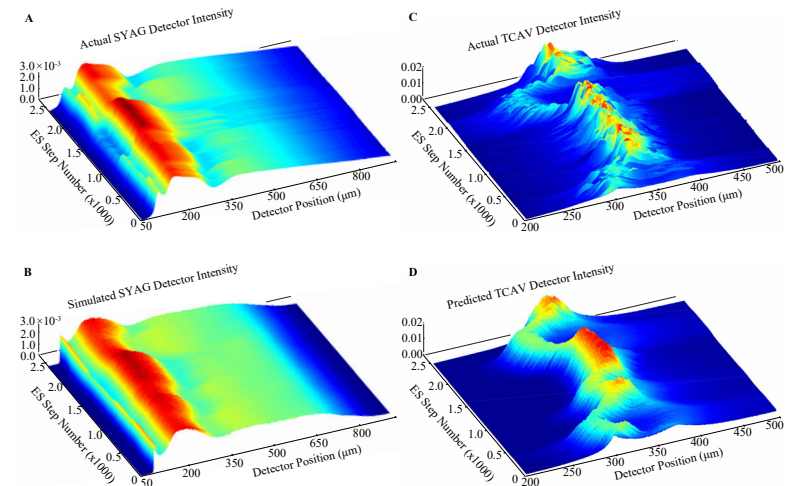
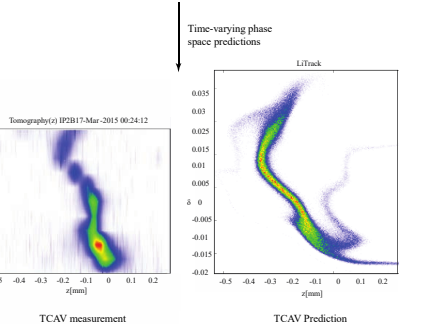
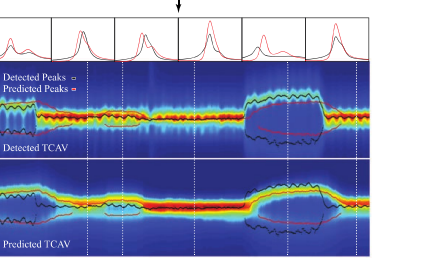
FACET: E-bunch profile prediction based on non-destructive measurements of energy spread spectrum. A. Scheinker and S. Gessner, "Adaptive method for electron bunch profile prediction," *Physical Review Accelerators and Beams*, 18, 102801, 2015.



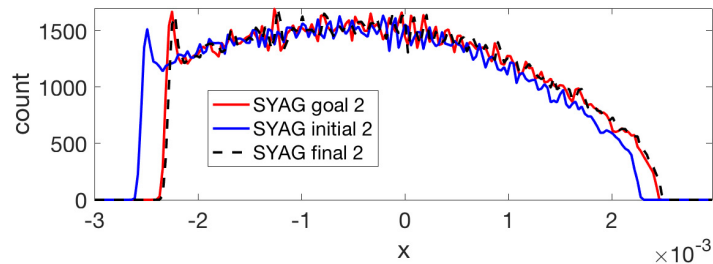
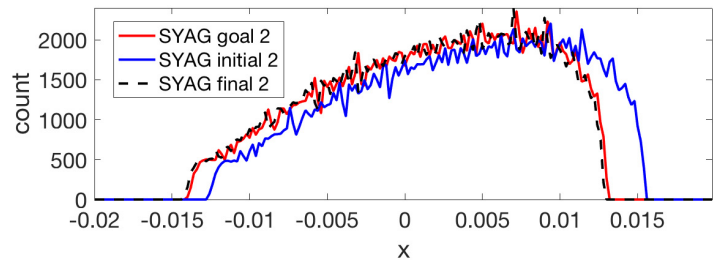
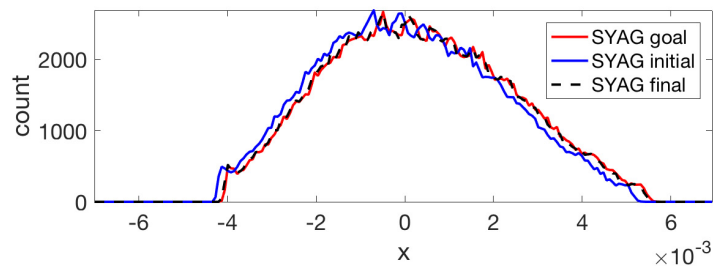
**FACET: E-bunch profile prediction based on non-destructive measurements of energy spread spectrum.
 A. Scheinker and S. Gessner,
 “Adaptive method for electron bunch profile prediction,”
 Physical Review Accelerators and Beams, 18, 102801, 2015.**



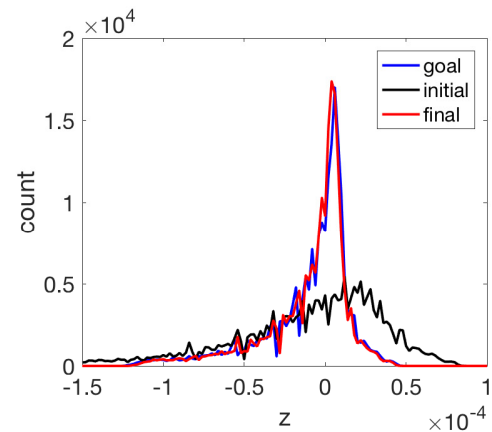
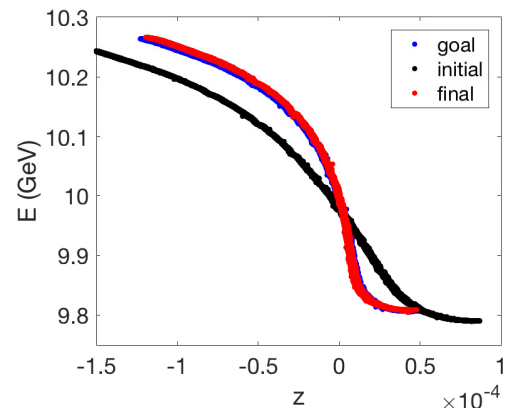
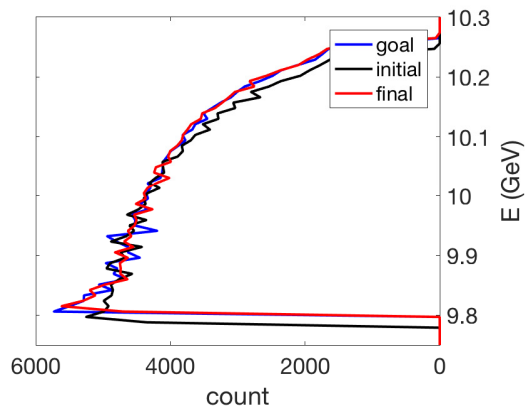
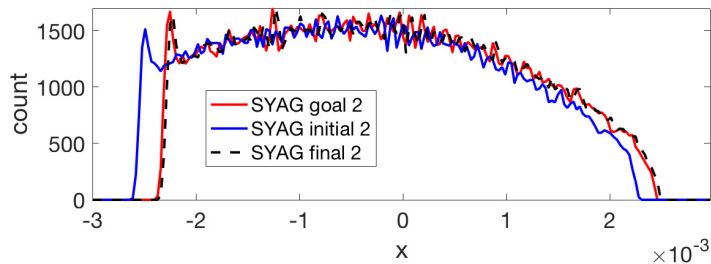
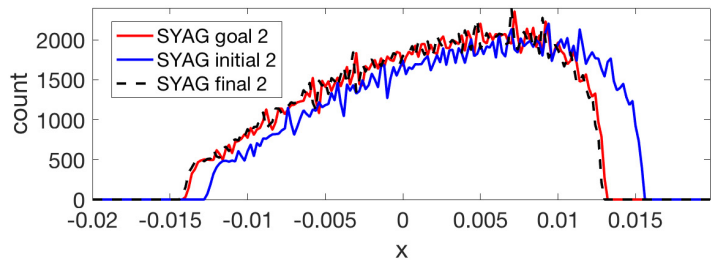
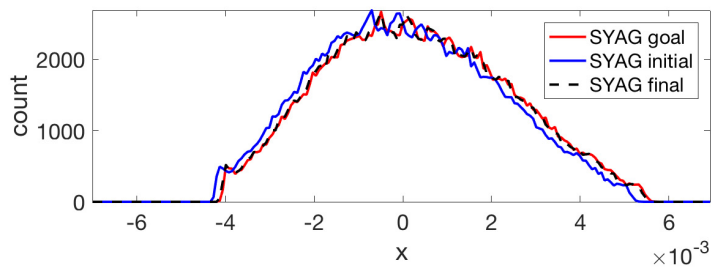
Parameters iteratively tuned to match simulated energy spread spectrum to actual detected spectrum.



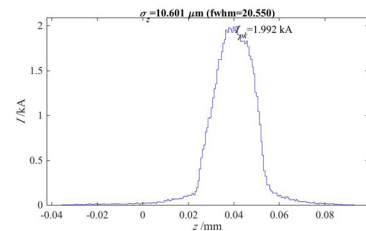
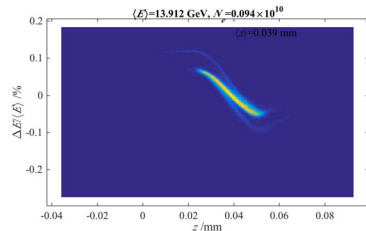
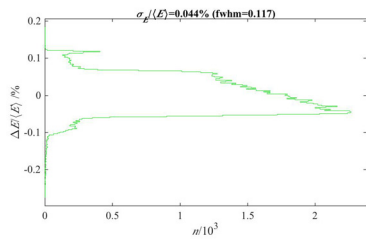
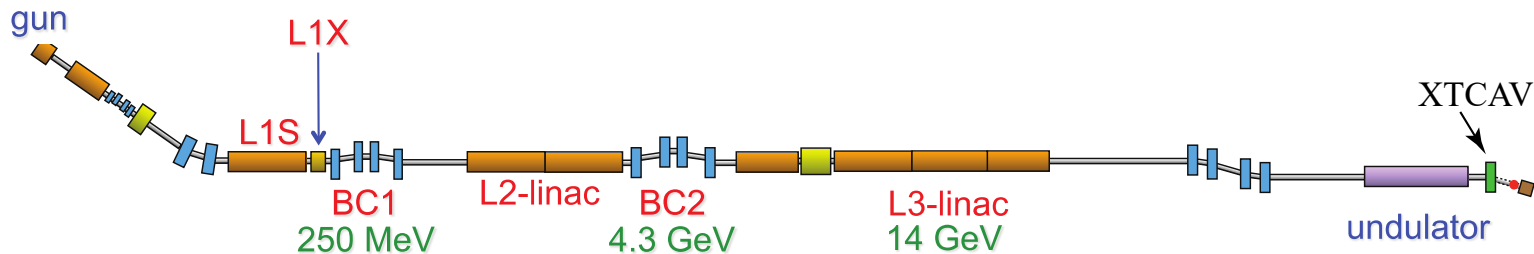
FACET-II Virtual Diagnostics and Phase Space Control: Adjusting RF phases to match energy spread



FACET-II Virtual Diagnostics and Phase Space Control: Adjusting RF phases to match energy spread spectrums



LCLS automatic longitudinal phase space tuning. A. Scheinker. and D Bohler, "Demonstration of model-independent control of the longitudinal phase space of electron beams in the LCLS with fs resolutions," *submitted*.

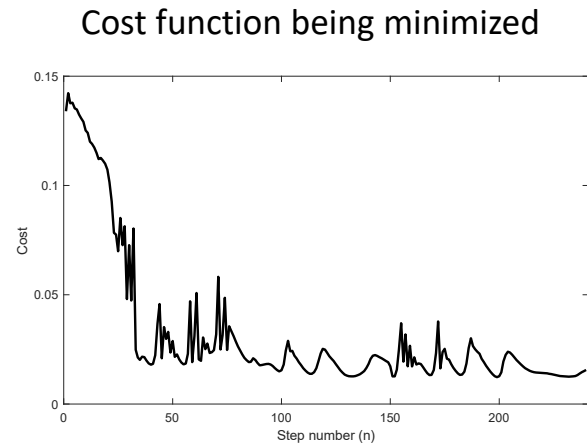
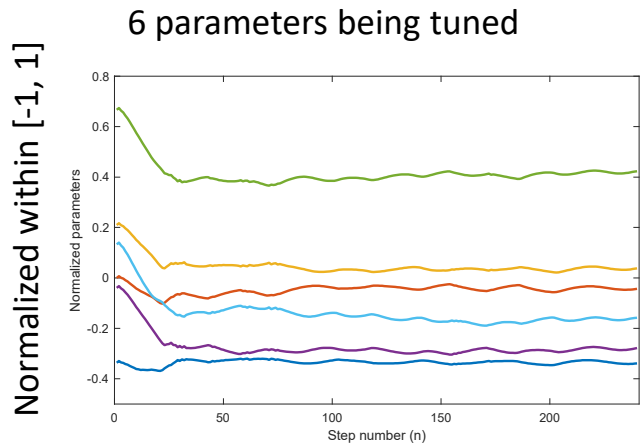


Energy Spread

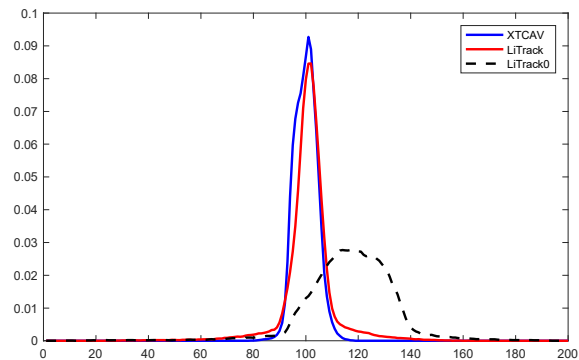


Longitudinal charge density distribution

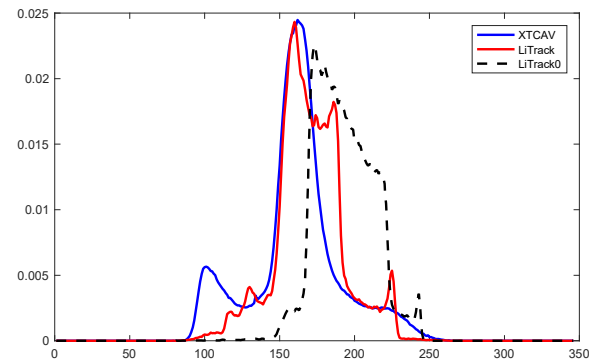




Longitudinal charge density distribution

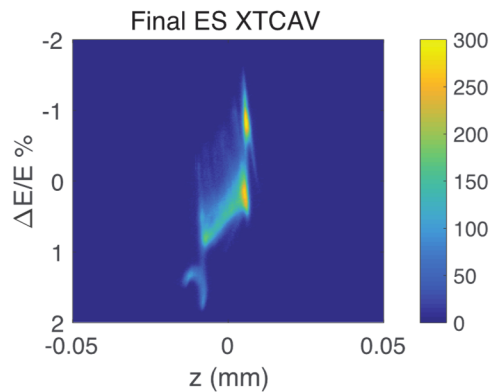
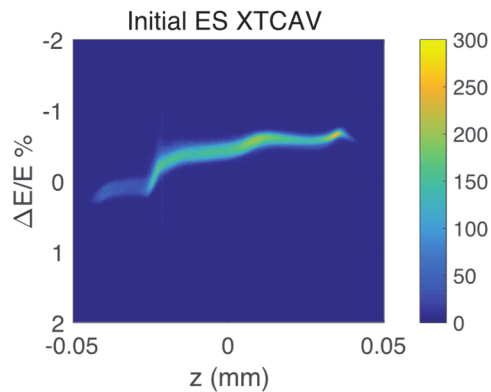
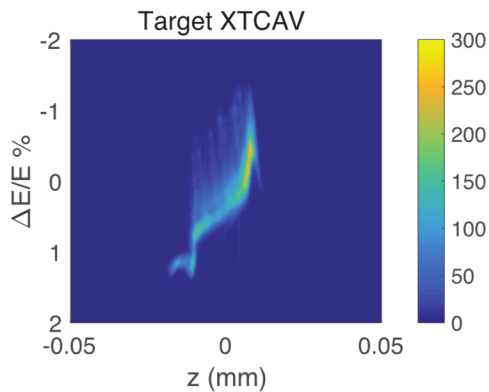
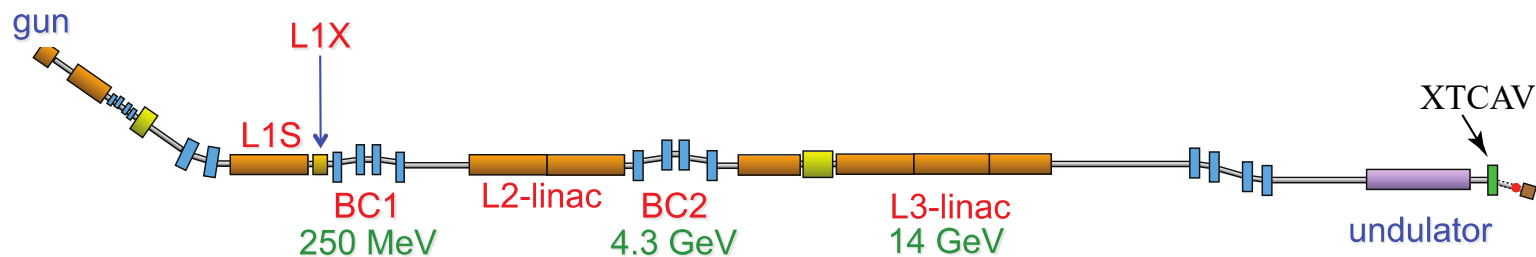


Energy Spread

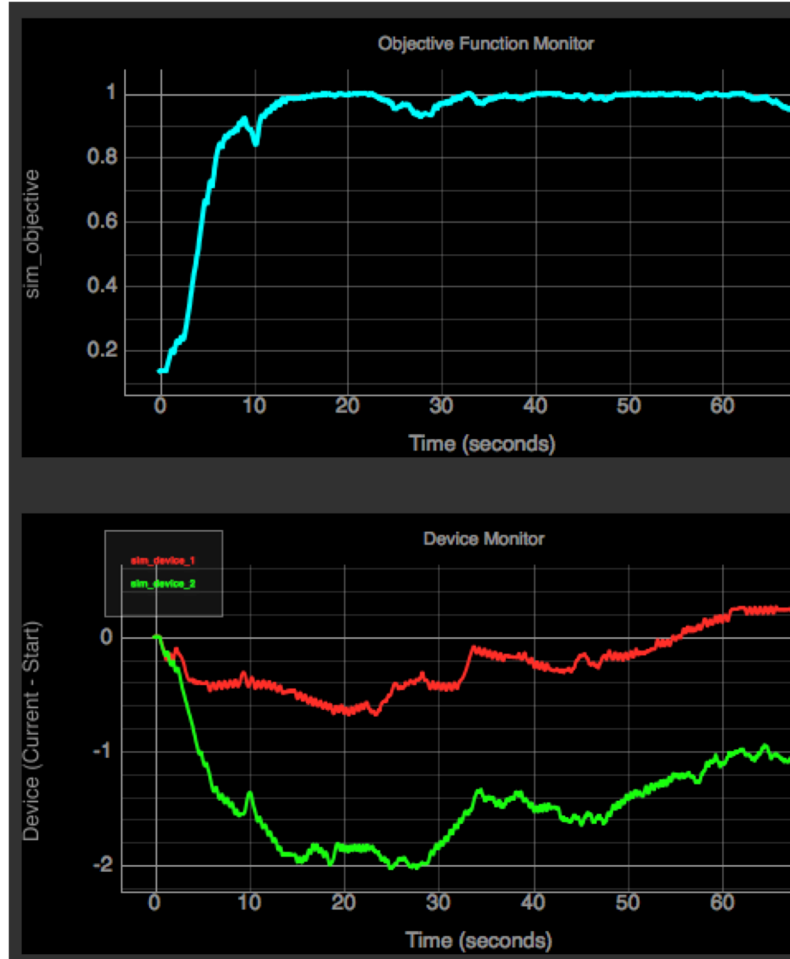


----- LiTrackES initial
 ————— LiTrackES final
 ————— Goal

LCLS automatic longitudinal phase space tuning. A. Scheinker. and D Bohler, "Demonstration of model-independent control of the longitudinal phase space of electron beams in the LCLS with fs resolutions," *submitted*.

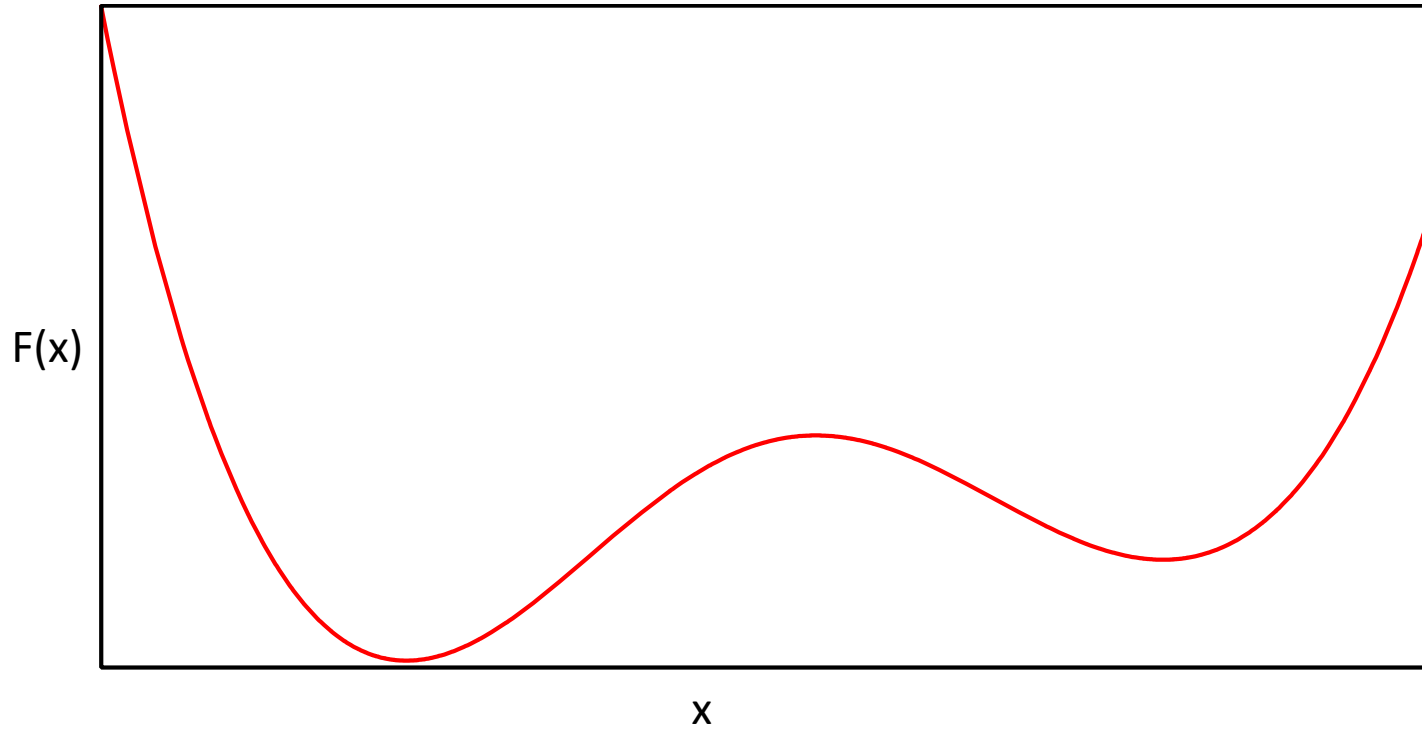


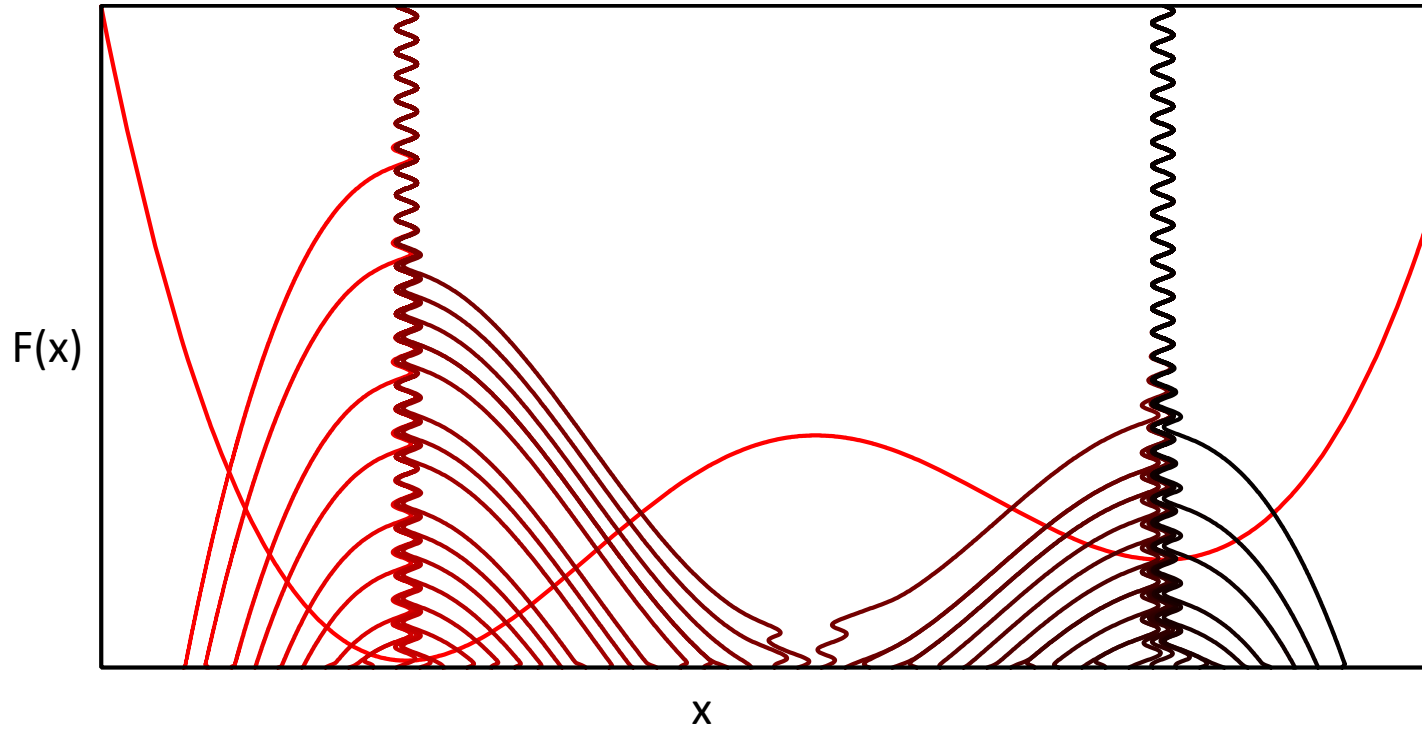
ES in OCELOT for time-varying systems

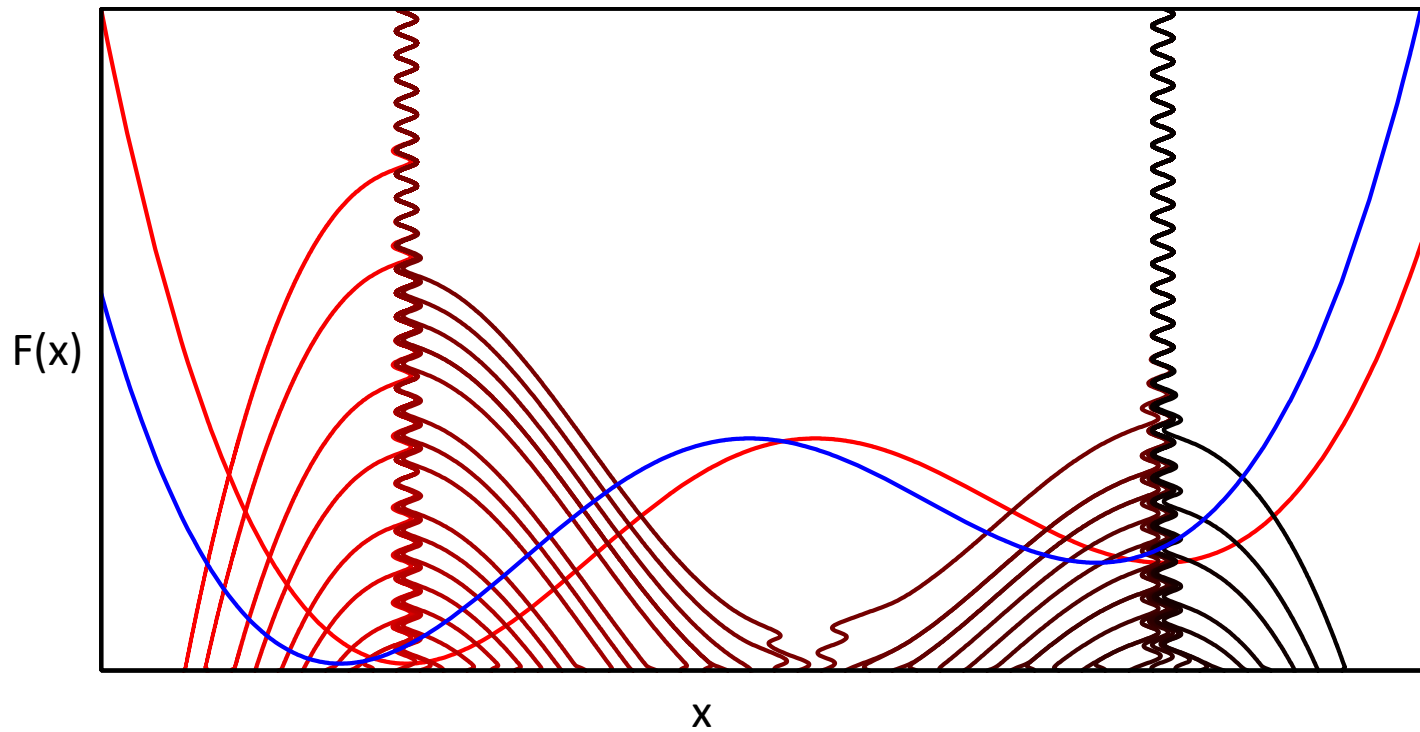


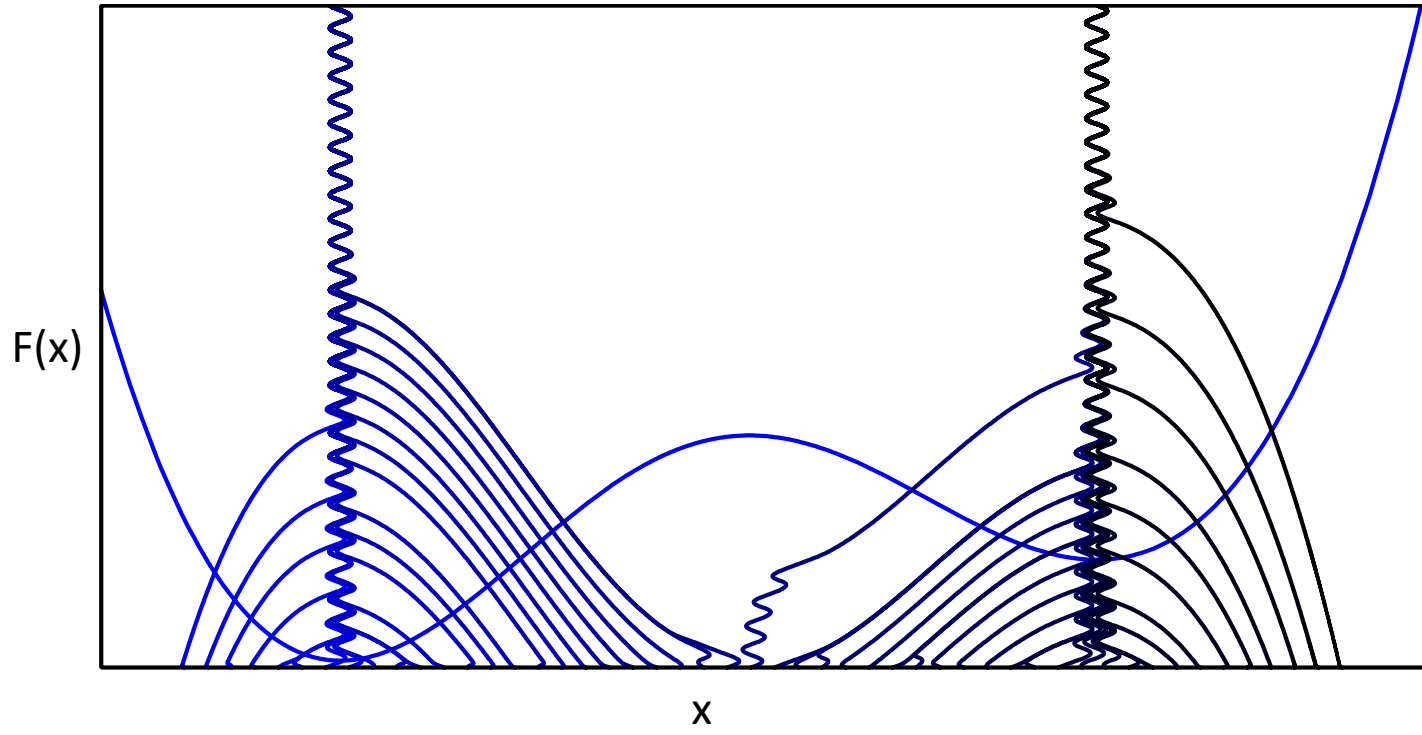
Combining ML and ES

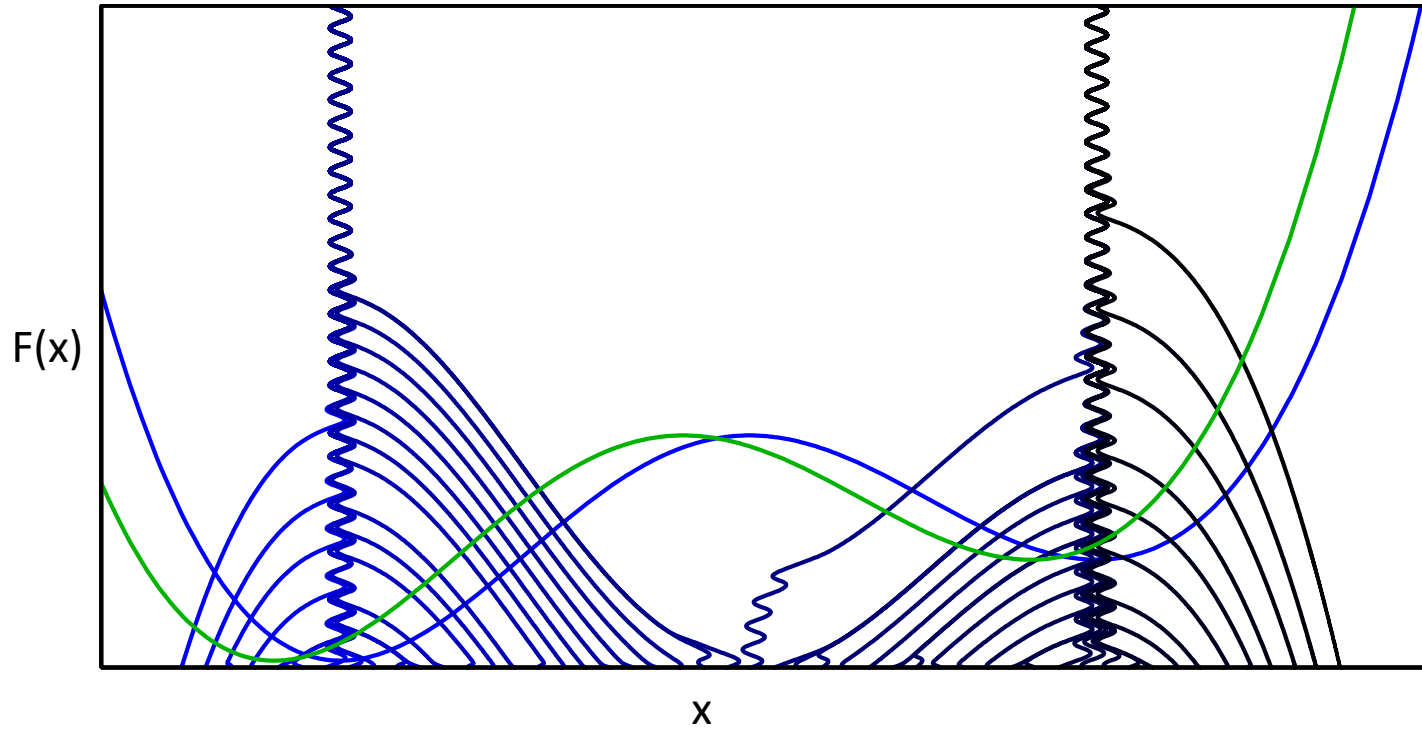
(LANL and SLAC)

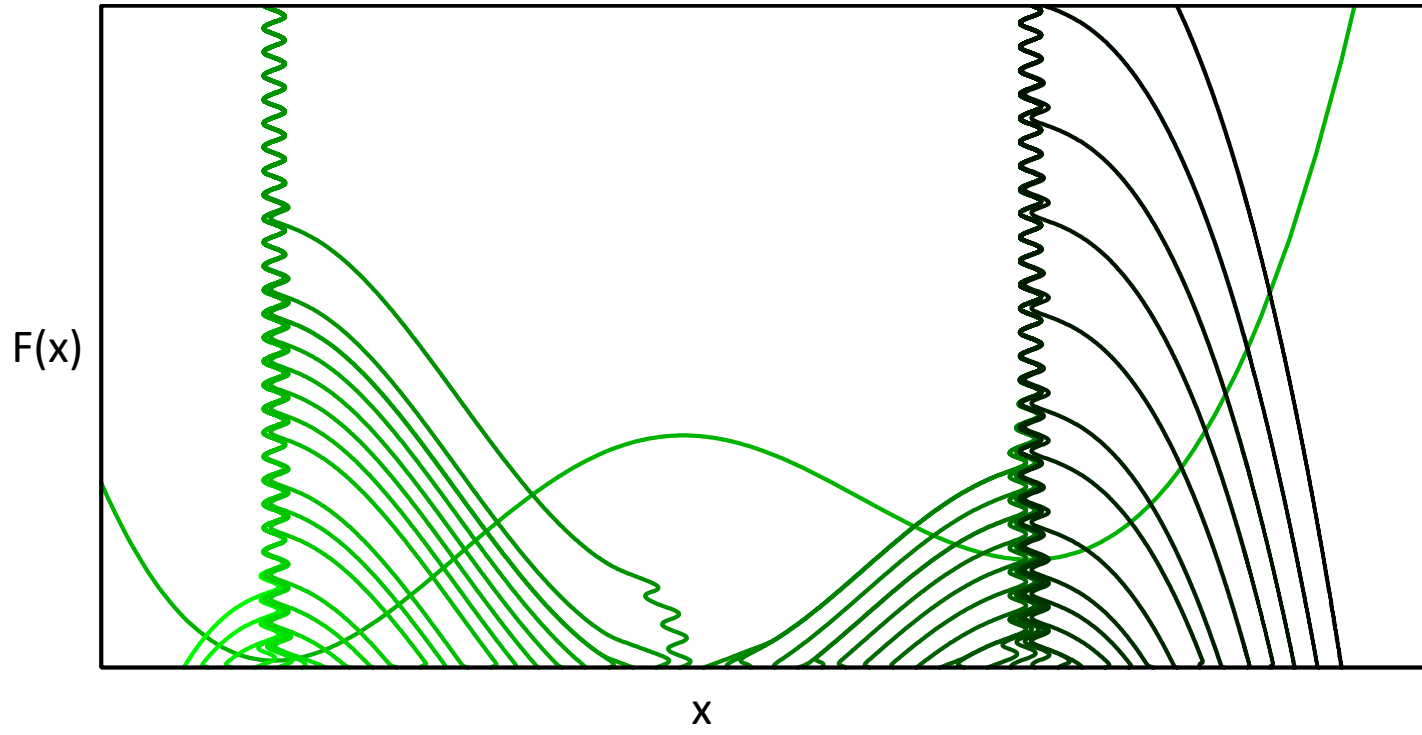


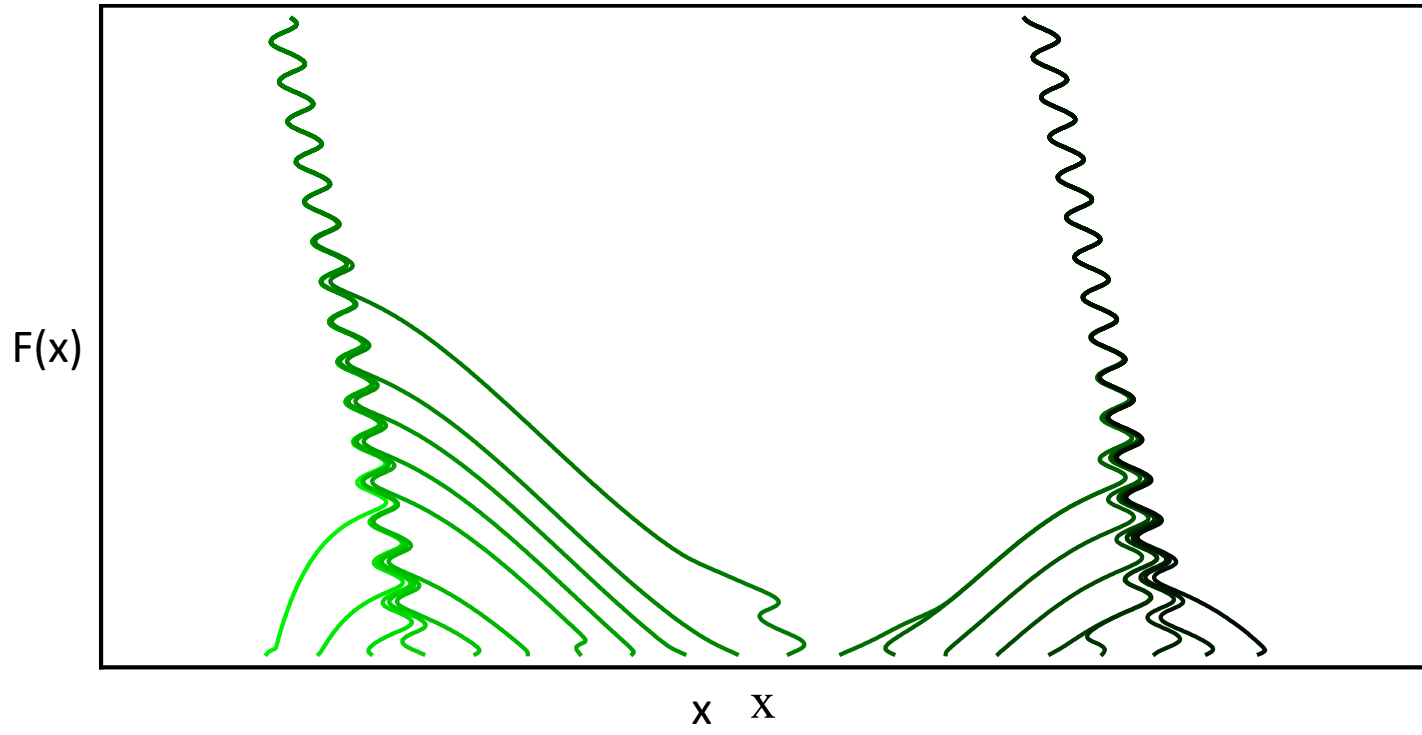




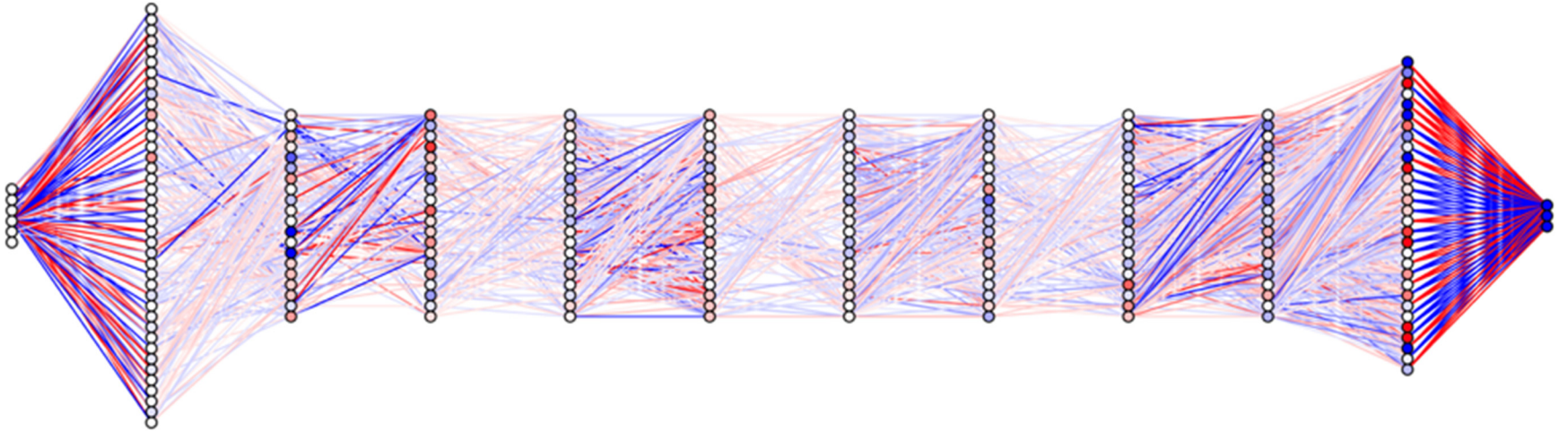








Re-training a deep NN with many output nodes would take too long



Ongoing work

